

Accepted Manuscript

Novel non-sulfonamide 5-HT₆ receptor partial inverse agonist in a group of imidazo[4,5-*b*]pyridines with cognition enhancing properties

David Vanda, Miroslav Soural, Vittorio Canale, Severine Chaumont-Dubel, Grzegorz Satała, Tomasz Kos, Petr Funk, Veronika Fülöpová, Barbora Lemrová, Paulina Koczurkiewicz, Elżbieta Pękala, Andrzej J. Bojarski, Piotr Popik, Philippe Marin, Paweł Zajdel

PII: S0223-5234(17)31084-X

DOI: [10.1016/j.ejmech.2017.12.053](https://doi.org/10.1016/j.ejmech.2017.12.053)

Reference: EJMECH 10031

To appear in: *European Journal of Medicinal Chemistry*

Received Date: 4 November 2017

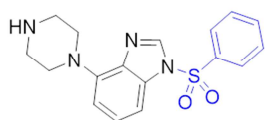
Revised Date: 9 December 2017

Accepted Date: 14 December 2017

Please cite this article as: D. Vanda, M. Soural, V. Canale, S. Chaumont-Dubel, G. Satała, T. Kos, P. Funk, V. Fülöpová, B. Lemrová, P. Koczurkiewicz, Elż. Pękala, A.J. Bojarski, P. Popik, P. Marin, Paweł. Zajdel, Novel non-sulfonamide 5-HT₆ receptor partial inverse agonist in a group of imidazo[4,5-*b*]pyridines with cognition enhancing properties, *European Journal of Medicinal Chemistry* (2018), doi: 10.1016/j.ejmech.2017.12.053.

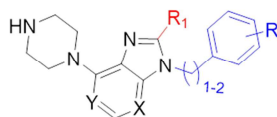
This is a PDF file of an unedited manuscript that has been accepted for publication. As a service to our customers we are providing this early version of the manuscript. The manuscript will undergo copyediting, typesetting, and review of the resulting proof before it is published in its final form. Please note that during the production process errors may be discovered which could affect the content, and all legal disclaimers that apply to the journal pertain.





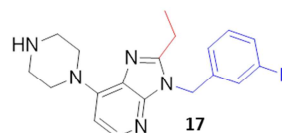
- Scaffold hopping
- Bioisosteric replacement

Design



- Solid-phase synthesis
- Solution-phase synthesis

Synthesis



17

partial inverse agonist

K_i (5-HT₆) = 6 nM; IC₅₀ = 17.6 nM;
NORT (SCOP) = 0.1 mg/kg + 0.3 mg/kg Donepezil, *p.o.*

Pharmacological evaluation

ACCEPTED MANUSCRIPT

Novel non-sulfonamide 5-HT₆ receptor partial inverse agonist in a group of imidazo[4,5-b]pyridines with cognition enhancing properties

David Vanda,^a Miroslav Soural,^a Vittorio Canale,^b Severine Chaumont-Dubel,^c Grzegorz Satała,^d
Tomasz Kos,^e Petr Funk,^f Veronika Fülöpová,^a Barbora Lemrová,^f Paulina Koczurkiewicz,^g
Elżbieta Pękala,^g Andrzej J. Bojarski,^d Piotr Popik,^e Philippe Marin,^c Paweł Zajdel^{b,*}

^a*Institute of Molecular and Translational Medicine, Faculty of Medicine and Dentistry, Palacký University, 5 Hněvotínská Street, 779-00 Olomouc, Czech Republic*

^b*Department of Medicinal Chemistry, ^gDepartment of Pharmaceutical Biochemistry, University Medical College, 9 Medyczna Street, 30-688 Kraków, Poland*

^c*Institut de Génomique Fonctionnelle, CNRS UMR 5203, INSERM U1191 Université de Montpellier, Montpellier Cedex 5, France*

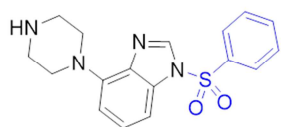
^f*Department of Organic Chemistry, Faculty of Science, Palacký University, 12 17.listopadu Street, 771-46 Olomouc, Czech Republic*

^d*Department of Medicinal Chemistry, ^eDepartment of Drug Development, Institute of Pharmacology, Polish Academy of Sciences, 12 Smętna Street, 31-343 Kraków, Poland*

*Corresponding author:

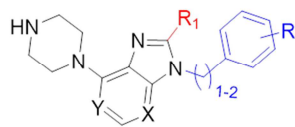
Department of Medicinal Chemistry
Jagiellonian University Medical College
e-mail: pawel.zajdel@uj.edu.pl
Tel.: +48 12 620 54 50; fax: +48 12 620 54 05

Graphical abstract



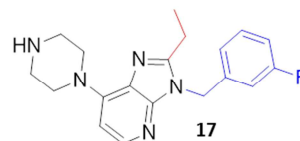
- Scaffold hopping
- Bioisosteric replacement

Design



- Solid-phase synthesis
- Solution-phase synthesis

Synthesis



17

partial inverse agonist

K_i (5-HT₆) = 6 nM; IC₅₀ = 17.6 nM;
NORT (SCOP) = 0.1 mg/kg + 0.3 mg/kg Donepezil, *p.o.*

Pharmacological evaluation

ACCEPTED MANUSCRIPT

Abstract

A small library of novel 3*H*-imidazo[4,5-*b*]pyridine and 3*H*-imidazo[4,5-*c*]pyridine derivatives was designed and synthesized as non-sulfonamide 5-HT₆ receptor ligands. *In vitro* evaluation allowed to identify compound **17** (2-ethyl-3-(3-fluorobenzyl)-7-(piperazin-1-yl)-3*H*-imidazo[4,5-*b*]pyridine) as potent 5-HT₆ receptor partial inverse agonist in G_s signaling ($K_i = 6$ nM, $IC_{50} = 17.6$ nM). Compound **17** displayed high metabolic stability, favorable cytochrome P450 isoenzyme (2D6, 3A4) profile, did not affect PgP-protein binding, without evoking mutagenic effects. It was orally bioavailable and brain penetrant. In contrast to intepirdine (SB-742457), which prevented 5-HT₆R-elicited neurite growth and behaved as an inverse agonist of cyclin-dependent kinase 5 (Cdk5), compound **17** has no influence on neuronal differentiation. Compound **17** exerted significant pro-cognitive properties in novel object recognition (NOR) task in rats reversing both phencyclidine- and scopolamine-induced memory deficits (MED = 1 and 0.3 mg/kg, *p.o.*, respectively). These effects were similar to those produced by intepirdine. Additionally, combination of inactive doses of compound **17** (0.1 mg/kg) and donepezil (0.3 mg/kg) produced synergistic effect to reverse scopolamine-induced memory deficits. Accordingly, investigating putative divergence between inverse agonists and neutral antagonists as cognitive enhancers in neurodegenerative and psychiatric disorders is certainly of utmost interest.

Keywords: 3*H*-imidazo[4,5-*c*]pyridine, imidazo[4,5-*c*]pyridines, solid-supported synthesis, 5-HT₆ receptor inverse agonist, Cdk5 signaling, intepirdine, novel-object recognition test, phencyclidine, scopolamine, donepezil, pro-cognitive activity, dementia, neurodegenerative disorders.

1. Introduction

The serotonin 5-HT₆ receptor (5-HT₆R) belongs to the superfamily of G protein-coupled receptors (GPCRs). It is canonically coupled to Gs protein, promoting cAMP formation. 5-HT₆R also engage the extracellular signal-regulated kinase (ERK)1/2 pathway *via* the Src-family tyrosine kinase Fyn [1] and the mammalian target of rapamycin (mTOR) pathway known to be involved in brain development, learning, and synaptic plasticity [2]. Moreover, 5-HT₆R recruit a network of proteins that includes cyclin-dependent kinase 5 (Cdk5) and some of its substrates, which control various neurodevelopmental processes [3].

The 5-HT₆R is exclusively localized in the central nervous system, predominantly in hippocampus, striatum, nucleus accumbens and prefrontal cortex. Its enrichment in those brain regions suggests an important role in memory and cognition processes [4,5]. These findings were further supported by a large body of evidence indicating that 5-HT₆R blockade improves cognitive performance by enhancing cholinergic, glutamatergic and monoaminergic (e.g., dopaminergic and adrenergic) neurotransmissions in several rodent models of cognitive impairment [6,7]. Finally, pro-cognitive effects of two 5-HT₆R antagonists, idalopirdine (Lu-AE58054) and intepirdine (SB-742457) (Figure 1), were unequivocally demonstrated in Phase II clinical trials in patients with mild to moderate AD with treatment with the acetylcholine esterase inhibitor donepezil [8–10]. Intepirdine and another 5-HT₆R antagonist, landipirdine (Figure 1), are currently under evaluation in Phase II trials in patients with dementia with Lewy bodies and Parkinson's disease dementia, [11,12].

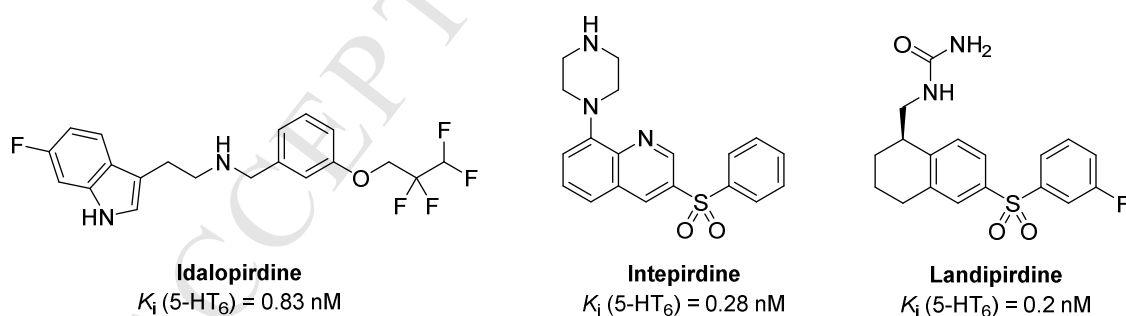


Figure 1. Chemical structure of 5-HT₆R antagonists evaluated in Phase II clinical trials.

Another important feature of 5-HT₆R, which depends on its association with interacting partners, is its high level of constitutive activity [13,14]. This underscores the need of developing ligands with neutral antagonist *vs.* inverse agonist properties in order to compare their pro-cognitive action in different paradigms of cognitive impairment.

Structural requirements for designing potent and selective 5-HT₆R ligands might be summarized into a positive ionizable nitrogen atom attached to a flat aromatic core ring system which is linked to a second distant aromatic ring mostly through a tetrahedral sulfonyl group [15,16]. The most recurrent chemical motif within 5-HT₆R ligands is represented by an indole moiety functionalized with *N*₁-arylsulfonyl fragment [17,18]. In consequence, several classes of 5-HT₆R ligands have been identified by scaffold hopping approach consisting in swapping carbon and nitrogen atom in an indole ring to generate benzimidazole, azaindole, indazole, azaindazole derivatives (Figure 2) [17,19,20].

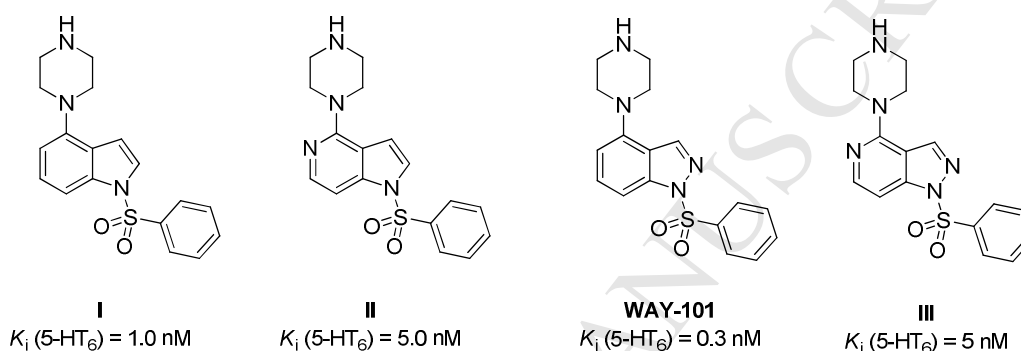


Figure 2. Chemical structure of 5-HT₆R ligands containing different indole-like scaffolds.

Only few efforts have been paid on replacing the sulfonyl group by its bioisosteric methylene group. This modification has either no influence on affinity of tryptamine derivatives for 5-HT₆R [16,21] or significantly decreased affinity of 3-(piperazin-1-ylmethyl)-1*H*-indole derivatives (Figure 3) [22].

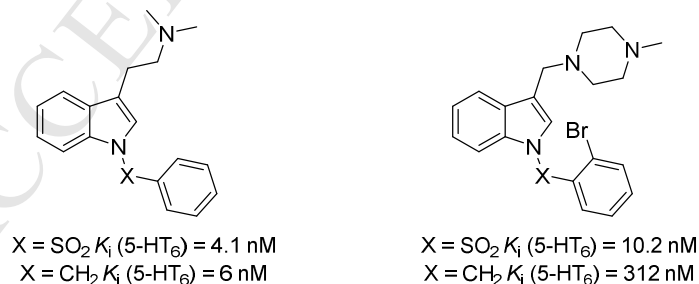


Figure 3. Comparison of the *in vitro* pharmacological activity of indole-type 5-HT₆R ligands.

Based on these findings, we applied a scaffold-hopping approach to design a novel *N*-benzyl 3*H*-imidazo[4,5-*b*] and 3*H*-imidazo[4,5-*c*]pyridine derivatives as potent and selective 5-HT₆R antagonists (Figure 4). To extend chemical diversity around imidazopyridines, structural modifications comprised an introduction of different alkyl/aryl substituents at C2-position at the

imidazole moiety, as well as the diversification at the *N*-benzyl fragment bearing electron donating or withdrawing substituents. Finally, a methylene linker between the benzyl fragment and the imidazo[4,5-*b*]pyridine was replaced by the ethylene one.

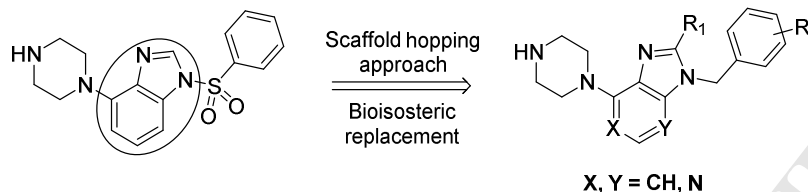


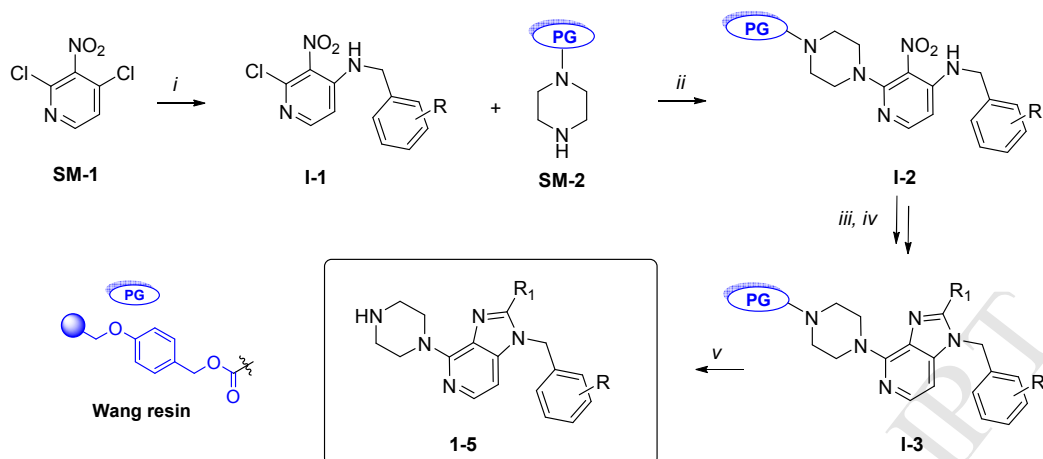
Figure 4. Design of a focused library of 3*H*-imidazo[4,5-*b*]pyridine and 3*H*-imidazo[4,5-*c*]pyridine derivatives using the scaffold hopping and *N*-benzyl replacement strategies.

In this study, we evaluated the *in vitro* affinity of synthesized compounds for 5-HT₆Rs, functional profile in Gs and Cdk5 paand selectivity panel, followed by ADMET and pharmacokinetic properties for the most promising derivative. Finally, the pro-cognitive activity of selected compound has been evaluated in the novel object recognition (NOR) task in rats by measuring its ability to reverse drug-induced memory deficits.

2. Results and Discussion

2.1. Chemistry

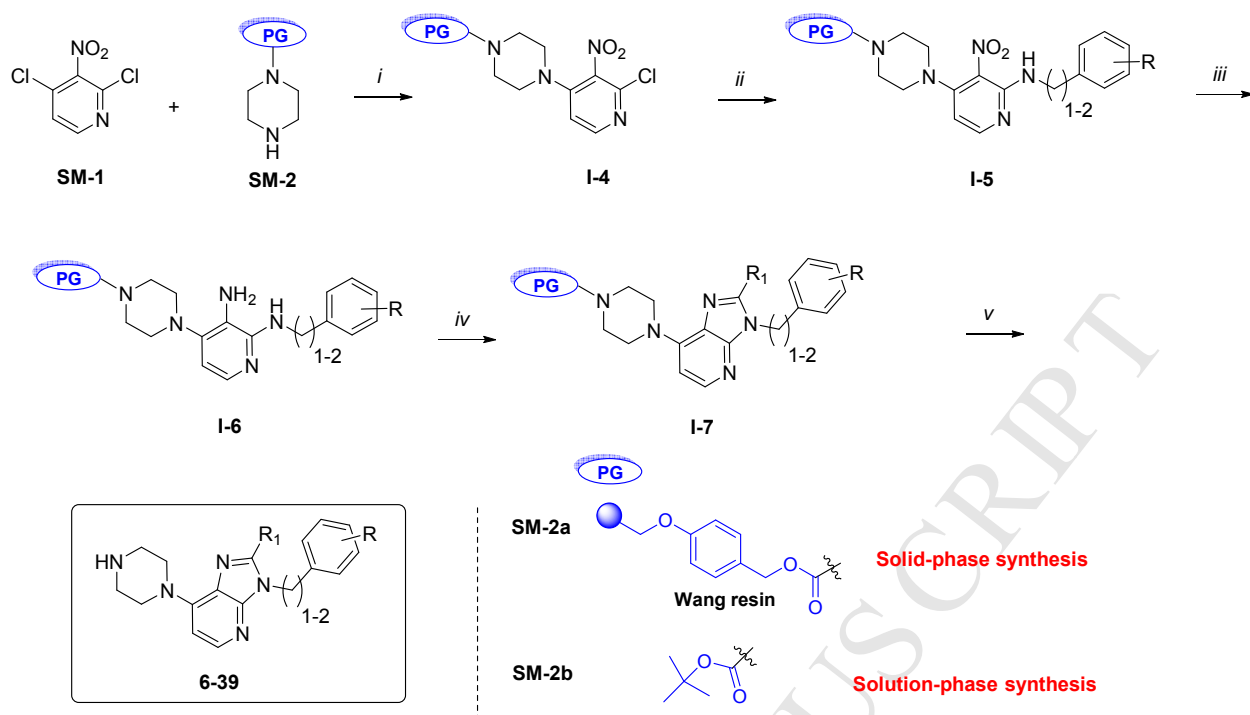
Target compounds were synthesized using either traditional solution-phase or solid-phase synthesis approach. For the preparation of imidazo[4,5-*c*]pyridines, a combined solution-phase/solid-phase synthesis approach was applied (Scheme 1) [23]. First, 2,4-dichloro-3-nitropyridine (**SM-1**) was reacted with selected benzylamines and the resulting intermediate **I-1** was immobilized using the resin capture with Wang-piperazine resin **SM-2**. Then, after reduction of the nitro group with sodium dithionite in a presence of phase-transfer catalyst, polymer supported imidazopyridines **I-2** were obtained using the thermal cyclization with aldehydes. Finally, target compounds **1-5** were cleaved from the resin **I-3** by treatment with a mixture of trifluoroacetic acid (TFA) in dichloromethane and purified with semi-preparative HPLC.



Scheme 1. Synthetic pathway used for the preparation of imidazo[4,5-*c*]pyridines **1-5** (overall yield 39–45%). Reagents and conditions: *i*) benzylamine, *N,N*-diisopropylethylamine (DIEA), dimethylsulfoxide (DMSO), rt, on; *ii*) DIEA, 70°C, on. *iii*) Na₂S₂O₄, K₂CO₃, tetrabutylammonium hydrogen sulfate (TBAHS), CH₂Cl₂/H₂O, rt, on; *iv*) aldehyde, DMSO, 80°C, on; *v*) TFA/ CH₂Cl₂ (50/50 v/v), rt, 1 h.

In contrast, the synthesis of imidazo[4,5-*b*]pyridines was totally performed on solid support (Scheme 2). First, piperazine was immobilized on Wang resin *via* carbamate functionality to yield **SM-2a** followed by the regioselective arylation with 2,4-dichloro-3-nitropyridine **SM-1** in the presence of *N,N*-diisopropylethylamine (DIEA). Resin **I-4** was then reacted with selected benzylamines in dimethylsulfoxide under mild conditions to yield intermediates **I-5**. Synthesis of target compounds **6–39** from intermediates **I-5** was accomplished using the same protocols as for solid-phase synthesis of imidazo[4,5-*c*]pyridines.

Phenethyl derivatives and selected benzyl derivatives including compound **17** chosen for behavioral evaluation were synthesized using solution-phase organic synthesis. The identical reaction pathway was used with Boc-piperazine **SM-2b** as starting material instead of the Wang-piperazine resin **SM-2a**. In some cases, the reaction conditions were slightly modified compared to solid-phase synthesis procedures (see Supp. Information for more details). In case of solution-phase synthesis, the Boc-protective group of final intermediates was cleaved using alcoholic hydrogen chloride and the final products were purified by crystallization.



Scheme 2. Synthetic pathway used for the preparation of imidazo[4,5-b]pyridines **6–39** (overall yield 30–42%). Reagents and conditions: For solid-phase synthesis: *i*) DIEA, DMSO, rt, on; *ii*) 10% amine in DMSO, rt, on; *iii*) Na₂S₂O₄, K₂CO₃, TBAHS, CH₂Cl₂/H₂O, rt, on; *iv*) aldehyde, DMSO, 80°C, on; *v*) TFA/ CH₂Cl₂ (50/50 v/v), rt, 1 h. For solution-phase synthesis: *i*) DIEA, DMSO, rt, 2 h; *ii*) amine, DMSO, DIEA, 80°C, 48 h; *iii*) Na₂S₂O₄, K₂CO₃, dimethylformamide (DMF)/H₂O, 80°C, 90 min; *iv*) aldehyde, DMF, 80°C, 48 h; *v*) HCl/MeOH or EtOH, rt, 48 h.

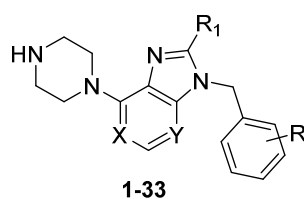
2.2. Structure-activity relationship studies

Evaluation of newly synthesized compounds **1–39** in [³H]-LSD binding experiments showed that they display high-to-low affinity for the 5-HT₆R ($K_i = 6–829$ nM) (Table 1). Structure-activity relationship studies focused first on a type of annelation of individual heterocyclic scaffolds showed that localization of the pyridine nitrogen atom is crucial for the binding to the 5-HT₆R: compounds bearing imidazo[4,5-*b*]pyridine fragment (pyridine nitrogen atom localized distal to the piperazine moiety) displayed higher affinity for 5-HT₆R than their imidazo[4,5-*c*]pyridine analogs having pyridine nitrogen atom localized proximal to the piperazine moiety (**6** vs **1** and **8** vs **3** and **23** vs **5**).

In an attempt to verify the limit in size and shape of the receptor binding cavity, to what extent it affects affinity of synthesized ligands for 5-HT₆R, the C2-position of imidazo[4,5-*b*]pyridine moiety was functionalized with different small or bulky alkyl/aryl substituents. Generally, the presence of alkyl substituents in C2-position slightly increases the affinity of compounds for the

tested receptor, compared with non-substituted derivatives (**7** vs **12**, **18** and **23**). In particular, the length of alkyl chain influenced the interaction with 5-HT₆R, with ethyl group being preferred over a methyl one (**8** vs **15**, **9** vs **16** and **12** vs **18**). Additionally, the replacement of small alkyl substituents with symmetric, sterically-hindered ones (i.e., isopropyl or 3-pentyl group) has not significantly impacted the affinity of the tested compounds for 5-HT₆R (**12** and **18** vs **23** and **28**; **17** vs **22** and **11** vs **29**). In contrast, bulky asymmetric substituents such as neopentyl group or aromatic fragments (i.e., 2-thienyl, 4-F-phenyl) were not tolerated, as they reduced the affinity for 5-HT₆R up to 12-fold (**11** vs **30**; **7** vs **32** and **22** vs **33**). This might result from the increased volume of the substituents, which affects access of compounds in the receptor binding pocket. Furthermore, selected substituents with different electronic properties at the *N*-benzyl fragment were investigated. Results revealed that the presence of substituent in position-3 was preferential for the binding to 5-HT₆R and the following rank order 3 position > non-substituted > 2 ≈ 4 position was observed. Moreover, the nature of the substituent at the *N*-benzyl fragment was highly relevant for the binding to the receptor.

Since many years, halogen atoms have been routinely used in drug optimization to improve affinity and biological activity mediated by given target, due to the ability of halogens to form additional interactions i.e., dipole-dipole (Cl, Br and I), and Van der Waals (F atoms). Consistent with these findings, compounds containing 3-F (**17** and **22**) and 3-Cl (**18** and **23**) substituents were the most potent among the newly synthesized compounds ($K_i < 20$ nM). In contrast, introduction of the strong electron withdrawing substituent 3-CF₃ slightly decreased the affinity for 5-HT₆R (**12** vs **13**). Moreover, mono-fluorinated compounds were preferred to di-fluorinated analogs for the binding to 5-HT₆Rs (**17** vs **19** and **20**). Replacement of the halogen atoms with weakly electron donating substituents (i.e., 3-methyl) maintained high affinity for the biological target (**12** vs **11** and **29** vs **28**), while the introduction of strong electron donating group (i.e., 2- or 3-methoxy) destabilized the ligand-receptor complex (**10**, **24** and **31**, $K_i = 337$, 92 and 165 nM, respectively).

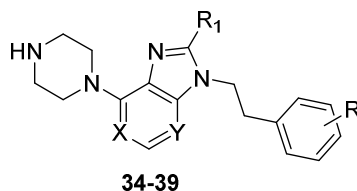
Table 1. The binding data of the synthesized compounds **1–33** for 5-HT₆R_s

Compd	X	Y	R ₁	R	K _i [nM] ^a 5-HT ₆
1	N	CH	H	H	450
2	N	CH	H	3-Cl	320
3	N	CH	Methyl	H	374
4	N	CH	Methyl	3-Cl	254
5	CH	N	Isopropyl	3-Cl	126
6	CH	N	H	H	110
7	CH	N	H	3-Cl	33
8	CH	N	Methyl	H	101
9	CH	N	Methyl	2-Cl	829
10	CH	N	Methyl	2-OMe	337
11	CH	N	Methyl	3-Me	26
12	CH	N	Methyl	3-Cl	21
13	CH	N	Methyl	3-CF ₃	62
14	CH	N	Methyl	4-F	317
15	CH	N	Ethyl	H	36
16	CH	N	Ethyl	2-Cl	177
17	CH	N	Ethyl	3-F	6
18	CH	N	Ethyl	3-Cl	7
19	CH	N	Ethyl	2,5-diF	57
20	CH	N	Ethyl	3,4-diF	139
21	CH	N	Isopropyl	2-F	61
22	CH	N	Isopropyl	3-F	13
23	CH	N	Isopropyl	3-Cl	20
24	CH	N	Isopropyl	3-OMe	92
25	CH	N	Isopropyl	4-F	80
26	CH	N	Isopropyl	4-Cl	107
27	CH	N	3-Pentyl	2-Cl	108
28	CH	N	3-Pentyl	3-Cl	30
29	CH	N	3-Pentyl	3-Me	42
30	CH	N	Neopentyl	3-Me	142
31	CH	N	Neopentyl	3-OMe	165
32	CH	N	2-Thienyl	3-Cl	165
33	CH	N	4-F-Phenyl	3-F	162

^a Mean K_i values (SEM ± 19%) based on three independent binding experiments

Having identified the preferential substitution pathway at the *N*-benzyl fragment (3-F and 3-Cl) and at the C2-position of imidazopyridine ring (methyl, ethyl, isopropyl), we then focused on the influence of an elongation of the *N*₁-methylene linker on the interaction with the 5-HT₆R.

Table 2. The binding data of the synthesized compounds **34–39** for 5-HT₆R_s



Compd	R ₁	R	K _i [nM] ^a 5-HT ₆
34	H	F	1298
35	H	Cl	1251
36	Me	Cl	312
37	Ethyl	F	56
38	Ethyl	Cl	42
39	Isopropyl	Cl	80

^a Mean K_i values (SEM ± 17%) based on three independent binding experiments

Binding data outlined in Table 2 showed that this modification decreased the affinity of the corresponding ligands for 5-HT₆R up to 4-fold (**12** vs **36**, **17** vs **37**). In line with the results obtained in the *N*-benzyl series, the following rank order among substitution patterns in C2-position at the imidazole moiety was found: ethyl > isopropyl > methyl >> H.

2.3. Extended *in vitro* pharmacology and functional activity evaluation

In the next step, selected compounds with the highest affinity for 5-HT₆R ($K_i < 25$ nM) were tested for their affinity for other serotonin (5-HT_{1A}, 5-HT_{2A}, 5-HT₇) and dopamine D₂ receptors. In contrast to clinically tested 5-HT₆R antagonists, which also possess high affinity for 5-HT_{2A}R, selected compounds displayed low affinity for this site ($K_i > 440$ nM) and high selectivity (up to 113-fold) against the other serotonin and dopaminergic receptor subtypes tested (Table 3).

Table 3. The antagonist activity of selected compounds for 5-HT₆R and their binding data for 5-HT_{1A}, 5-HT_{2A}, 5-HT₆ and D₂Rs.

Compd	K_i [nM] ^a	IC ₅₀ [nM] ^b	K_i [nM] ^a			
			5-HT _{1A}	5-HT _{2A}	5-HT ₇	D ₂
17	6	17.6	2790	441	12340	3482
18	7	51.9	1354	449	8748	6100
22	13	69.5	5934	475	11920	3436
23	20	56.4	2277	694	7139	2941
Intepirdine	1.4	2.8	2370	26	14230	997

^a Mean K_i values (SEM \pm 27%) based on three independent binding experiments

^b Mean IC₅₀ values (SEM \pm 18%) based on three independent experiments

We next evaluated the influence of the selected compounds on the 5-HT₆R constitutive activity at G_s signaling, in NG108-15 cells expressing recombinant receptors. In this cellular model a strong receptor constitutive activity was previously demonstrated [13]. The reference 5-HT₆R antagonist intepirdine (SB-742457) strongly decreased basal cAMP level in a concentration-dependent manner (IC₅₀ = 2.8 \pm 0.18 nM) and thus behaved as inverse agonist in this model (Figure 5). On the other hand, compounds **17**, **22**, and **23** only partially decreased cAMP level, and with lower apparent affinities, compared with intepirdine (IC₅₀: 17.6 \pm 2.1, 69.5 \pm 4.8, 56.4 \pm 3.4 nM, respectively) indicating that they behave as partial inverse agonists (Table 3). In contrast, compound **18** did not significantly affect cAMP level at any concentration tested, indicative of neutral antagonist properties at G_s signaling.

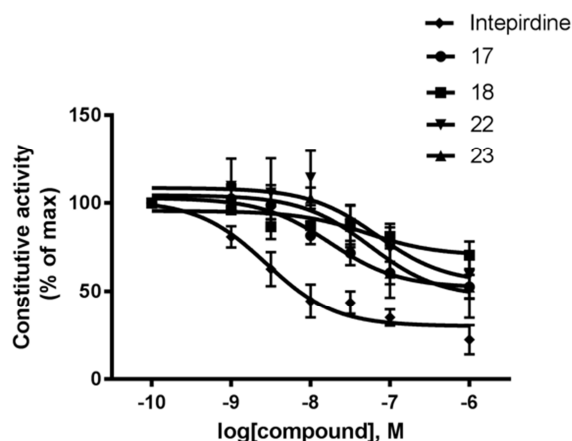


Figure 5. Influence of intepirdine and compounds **17**, **18**, **22**, and **23** on 5-HT₆R constitutive activity at G_s signaling in NG108-15 cells. Constitutive activity is represented as 100% of the activity measured in the absence of compound.

In addition to its established role in the control of cognition and mood, the 5-HT₆ receptor plays a key role in neuronal differentiation *via* its interaction with the Cdk5 protein kinase [13]. It was shown that expressing the 5-HT₆ receptor in NG108-15, a neuroblastoma cell line commonly used to investigate mechanisms underlying neuronal differentiation *in vitro*, induces a Cdk5-dependent NG108-15 cell differentiation, as assessed by measuring the length of neurites emitted by the cells 24 h after transfection. Consequently, Cdk5-dependent neurite growth can be inhibited by inverse agonists that disrupt the interaction between Cdk5 and the receptor. Reminiscent of its inverse agonist properties at G_s signalling, intepirdine strongly reduced NG-108-15 cell neurite length ($15.69 \pm 1.45 \mu\text{m}$, $n = 31$ cells *vs.* $58.61 \pm 3.52 \mu\text{m}$, $n = 32$ in vehicle-treated cells). In contrast, neurite length of cells treated with compound **17** ($51.84 \pm 3.07 \mu\text{m}$, $n = 104$ cells) was not different from control cells, indicating that this compound behaves as neutral antagonist at 5-HT₆ receptor-operated Cdk5 signalling (Figure 6).

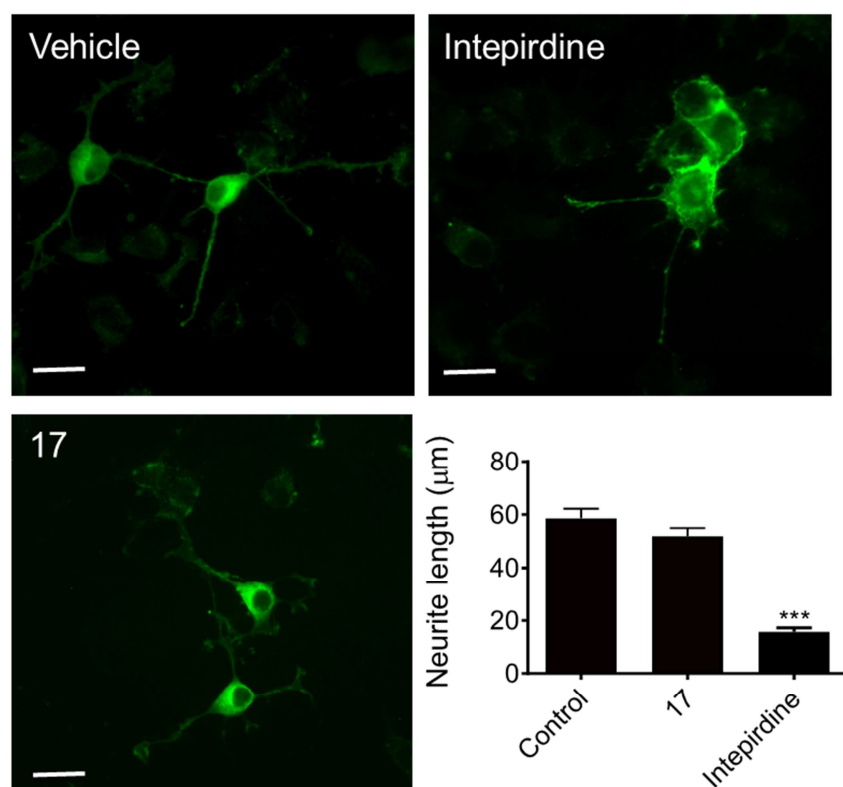


Figure 6. NG108-15 cells were transfected with a plasmid encoding a GFP-tagged 5-HT₆ receptor and exposed to either DMSO (Control) , intepirdine (1 µM) or compound **17** (1 µM) for 24 h. The histogram shows the means ± SEM of neurite length in each experimental condition measured from three independent experiments. *** p<0.001 vs. cells expressing 5-HT₆ receptor and treated with DMSO. Scale bar, 10 µm.

In line with these results, compound **17** was selected for further *in vitro* binding evaluation towards “off-target” receptor panel at CEREP displaying weak affinity for dopaminergic D₃ (18% @ 1 µM), and no adrenergic α₁ (0.2% @ 1 µM), histamine H₁ and H₃ (-4.9 and 1.6% @ 1 µM, respectively), muscarinic M₁ (3% @ 1 µM), and the serotonin transporter (SERT, 1.9% @ 1 µM). Finally, compound **17** did not bind at *h*ERG potassium channel (-6.1% @ 1 µM). These results suggested a low risk of tested compound to evoke undesirable cardiovascular (α₁, *h*ERG) or CNS (H₁) side effects. No affinity for M₁ receptor is favorable to observe the positive outcome in increase of acetylcholine via blockade of 5-HT₆R.

2.4. Preliminary ADMET properties evaluation

Early *in vitro* screening of ADMET parameters is essential in a drug discovery/lead optimization process to verify if a drug candidate displays desirable pharmacokinetics (PK) profiles that warrant further preclinical development.

Compound **17** was readily soluble in water (21.45 mg/mL; 50 mM), it displayed a low intrinsic clearance ($Cl_{int} = 1.73$ mL/min/kg), and a half-life counting $t_{1/2} = 100$ min in rat liver microsomes (RLM) assays. Next, the influence of **17** on liver human cytochrome CYP3A4 and CYP2D6 isozymes, which are responsible for the metabolism of about 40% of all marketed drugs, was assessed in order to exclude potential drug-drug interaction. No inhibition activity by compound **17** was detected in the CYP3A4 assay, but a slight induction of the CYP2D6 activity was observed at higher concentration (25 μ M) (Table 4).

Considering that compounds which are potential substrates of the glycoprotein P (P-gp) might be effluxed from the intestinal lumen as well as excluded from the brain resulting in poor bioavailability, the efflux ratio of compound **17** was evaluated in Caco-2-cell line. Experiments were performed at Eurofins Cerep according to the procedures reported online at www.cerep.fr. Compound **17** possessed a high permeability in this model indicating that it is not a P-gp substrate (Table 4).

Next, a preliminary pharmacokinetic profiling of compound **17** was determined in male Wistar rats injected with a single dose (10 mg/kg *p.o.*). This compound was rapidly absorbed and able to cross the blood-brain barrier with a C_{max} value reaching 139.7 ng/mL in the brain after 15 min (T_{max}). It was eliminated from the brain after 300 min.

In a view of toxicology and safety issues, the potential mutagenicity of compound **17** was further determined in Ames test. Evaluated compound displayed no mutagenic properties in two strains of *Salmonella typhimurium*, e.g. TA98 and TA100.

Table 4. Summary of the ADMET profile evaluation for compound **17**

Assay type	Compound 17
Solubility in H ₂ O	50 mM
Microsomal stability in RLM assay	Cl _{int} = 1.73 ml/min/kg
Cytochrome P450 inhibition (CYP3A4, CYP2D6)	No inhibition at tested concentration (0.025–25 μM)
Permeability	High, no substrate of P-gp
Ames test	Not mutagenic
PK	T _{max} = 15 min C _{max} = 139 ng/mL

2.5. Behavioral evaluation

In line with the ability of 5-HT₆R antagonists to induce pro-cognitive effects in the NOR task in various paradigms of cognitive impairment, we next evaluated the ability of compound **17** to rescue deficit in novel object recognition in rats treated with phencyclidine (PCP) or scopolamine (SCOP) [24]. As expected, vehicle-treated, but not phencyclidine (PCP, 5 mg/kg) and scopolamine (SCOP, 1.25 mg/kg)-treated, rats spent significantly more time exploring the novel object than the familiar one, indicating that both treatments abolished the ability to discriminate novel and familiar objects. These deficits were significantly reduced following administration of compound **17** (1 and 3 mg/kg) and intepirdine (0.3 and 1 mg/kg) (Figure 7), suggesting that tested compound **17** reversed PCP-induced cognitive impairment, being similar to the effects of intepirdine [25].

Furthermore, compound **17** (at 0.3 but not 0.1 mg/kg) and donepezil (at 1 but not 0.3 mg/kg) reversed the scopolamine-induced object recognition deficit (Figure 8). Because 5-HT₆R antagonists have been tested in clinical trials as a combination with donepezil [22,26], rats were also treated with an inactive dose of **17** (0.1 mg/kg) and donepezil (0.3 mg/kg). The cognitive performance of rats co-treated with inactive doses was comparable to the active dose (1 mg/kg) of donepezil given alone and to the vehicle-treated control group.

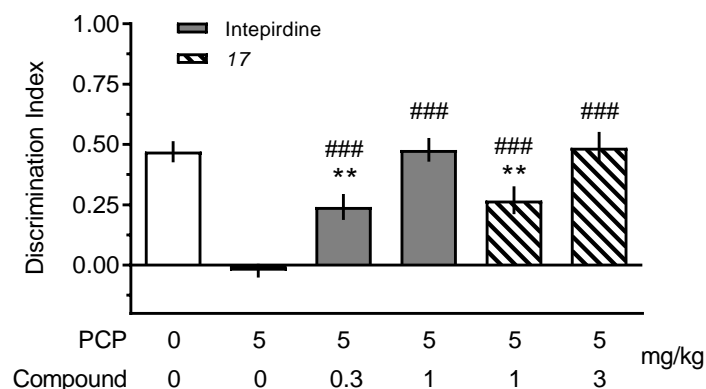


Figure 7. Effects of compound **17** on PCP-induced cognitive impairment in the novel-object recognition test in rats. The data are presented as the mean \pm SEM of discrimination index (DI). N = 8–10 of rats per group. One-way ANOVA demonstrated significant effects of treatment: $F(5, 48) = 17.1$; $P < 0.001$. Symbols: ** $P < 0.01$ vs vehicle-treated group; ### $P < 0.001$ vs PCP-treated group; Newman-Keuls multiple comparisons test.

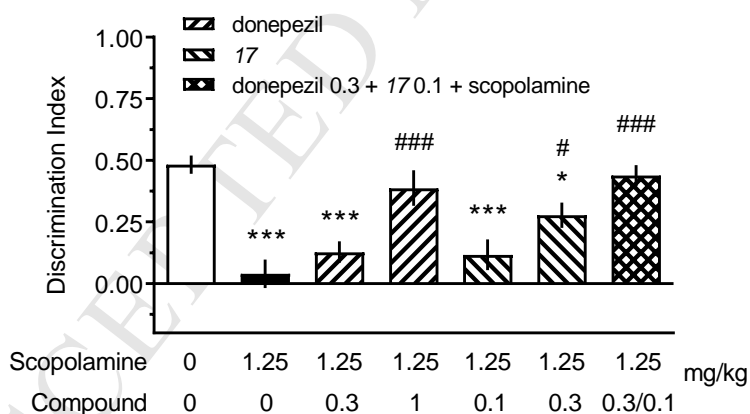


Figure 8. Effects of donepezil, compound **17**, and of co-administration of their inactive doses on scopolamine-induced cognitive impairment in the novel-object recognition test in rats. The data are presented as the mean \pm SEM of discrimination index (DI). N = 8–10 animals per group. One-way ANOVA demonstrated significant effects of treatment: $F(6, 59) = 11.15$; $P < 0.001$. Symbols: * $P < 0.05$, *** $P < 0.001$ vs vehicle-treated group; ### $P < 0.001$ vs scopolamine-treated group; Newman-Keuls multiple comparisons test.

3. Conclusion

By combining the concept of both scaffold hopping and isosteric replacement, a novel series of non-sulfonamide 5-HT₆R antagonists was designed and synthesized. Structure-activity relationship studies identified the structural features that favor interaction with the 5-HT₆R. Specifically, imidazo[4,5-*b*]pyridine scaffold was preferred over the imidazo[4,5-*c*]pyridine analog. Additionally, small alkyl substituents at the C2-position of imidazopyridine core accommodated better in the receptor binding pocket than bulkier alkyl or aromatic moieties. Finally, halogen atoms in 3-position at aryl moiety connected by methylene linker guaranteed the highest affinity for 5-HT₆R. The study identified compound **17** (2-ethyl-3-(3-fluorobenzyl)-7-(piperazin-1-yl)-3*H*-imidazo[4,5-*b*]pyridine) as new and potent 5-HT₆R partial inverse agonist at G_s signaling and neutral antagonist in Cdk5 pathway, displaying favorable ADMET profile. Due to its ability (alone or in combination with an inactive dose of donepezil) to reverse PCP- and SCOP-induced cognitive impairments in the NOR task, compound **17** might be considered as a pharmacological tool to further investigate the difference between partial inverse agonists and neutral antagonists as potential cognitive enhancers in neurodegenerative and genetic disorders.

4. Experimental Section

4.1. Chemistry

4.1.1. General Methods

Solvents and chemicals were purchased from Aldrich (Milwaukee, IL, www.sigmaaldrich.com) and Acros (Geel, Belgium, www.acros.cz). Wang resin (100-200 mesh, 1% DVB, 0.9 mmol/g) was obtained from AAPPTec (Louisville, KY, www.aapptec.com). Solid-phase synthesis was carried out in plastic reaction vessels (syringes, each equipped with a porous disk) using a manually operated synthesizer (Torviq, Niles, MI, www.torviq.com). All reactions were carried out at ambient temperature (21 °C) unless stated otherwise. The volume of wash solvent was 10 mL per 1 g of resin. For washing, resin slurry was shaken with the fresh solvent for at least 1 min before changing the solvent. Resin-bound intermediates were dried by a stream of nitrogen for prolonged storage and/or quantitative analysis. For the LC/MS analysis a sample of resin (~ 5 mg) was treated by TFA in CH₂Cl₂, the cleavage cocktail was evaporated by a stream of nitrogen, and cleaved compounds extracted into 1 mL of MeCN/H₂O (1/1). The LC/MS analyses were carried out on UHPLC-MS system consisting of UHPLC chromatograph Acquity with photodiode array detector and single quadrupole mass spectrometer (Waters), using X-Select C18 column at 30 °C and flow rate of 600 μ L/min. Mobile phase was (A) 0.01 M ammonium acetate in H₂O, and (B) MeCN, linearly programmed from 20% to 80% B over 2.5 min, kept for 1.5 min. The column was re-equilibrated with 20% of solution B for 1 min. The ESI I source operated at discharge current of 5 μ A, vaporizer temperature of 350 °C and capillary temperature of 200 °C. Purification of compounds synthesized by solid-phase synthesis was carried out on C18 reverse phase column (YMC Pack ODS-A, 20 \times 100 mm, 5 μ m particles), gradient was formed from 10 mM aqueous ammonium acetate and MeCN, flow rate 15 mL/min. For lyophilization of residual solvents (H₂O, ammonium acetate buffer, DMSO, DMF) at -110°C the ScanVac Coolsafe 110-4 was used.

All ¹H and ¹³C NMR experiments were performed with using JEOL ECA400II or ECX500 at magnetic field strengths of 9.39 T or 11.75 T corresponding to ¹H and ¹³C resonance frequencies of 399.78 MHz or 500.16 MHz and 100.53 MHz or 125.77 MHz at ambient temperature (25 °C) and/or higher temperature (50–150°C). Chemical shifts (δ) are reported in parts per million (ppm), and coupling constants (*J*) are reported in Hertz (Hz). The signal of DMSO-*d*₆ was set at 2.50 ppm in ¹H NMR spectra and at 39.5 ppm in ¹³C NMR spectra.

HRMS analysis was performed using LC-MS an Orbitrap Elite high-resolution mass spectrometer (Dionex Ultimate 3000, Thermo Exactive plus, MA, USA) operating at positive full scan mode (120 000 FWHM) in the range of 100-1000 *m/z*. The settings for electrospray ionization were as follows: oven temperature of 150 °C and source voltage of 3.6 kV. The acquired data were

internally calibrated with phthalate as a contaminant in MeOH (m/z 297.15909). Samples were diluted to a final concentration of 0.1 mg/mL in H₂O and MeOH (50/50, *v/v*). Before HPLC separation (column Phenomenex Gemini, 50 × 2.00 mm, 3 μm particles, C18), the samples were injected by direct infusion into the mass spectrometer using autosampler. Mobile phase was isocratic MeCN/isopropyl alcohol/0.01 M ammonium acetate (40/5/55) and flow 0.3 mL/min.

4.1.2. Synthesis procedure for the preparation of *N*-benzyl-2-chloro-3-nitropyridin-4-amines (**I-1**)

2,4-Dichloro-3-nitropyridine (300 mg; 1.56 mmol) was dissolved in DMSO (3 mL). Subsequently, DIEA (543 μL; 3.12 mmol, 2 eq) and appropriate amine were added (2 eq). The reaction solution was stirred overnight at room temperature. On the following day, another portion of DIEA (270 μL; 1.56 mmol, 1 eq) was added to the solution, and the resulting mixture was directly added to the resin **SM-2**.

4.1.3. Solid-Phase synthesis of imidazo[4,5-*b*]pyridines and imidazo[4,5-*c*]pyridines

4.1.3.1. Immobilization of piperazine on Wang resin (**SM-2**)

Wang resin (1 g, 0.9 mmol/g) was washed three times with dichloromethane (DCM). A solution of 1,1'-carbonyldiimidazole (CDI) (810 mg, 5.0 mmol) and pyridine (400 μL, 5.0 mmol) in 10 mL DCM was added and the resin slurry was shaken for 2 h at room temperature. The resin was then washed three times with DCM and a solution of piperazine (431 mg, 5.0 mmol) in 10 mL DCM was added. The slurry was shaken 3 h at room temperature and the resin was subsequently washed three times with DCM. Determination of loading: the sample of resin **SM-2** (~ 30 mg) was reacted with Fmoc-OSu (65 mg, 0.2 mmol) in DCM (0.5 mL) for 30 min at room temperature. The resin was washed three times with DCM, five times with MeOH, dried and divided into two samples (2 × 10 mg). Both samples were cleaved from the resin using TFA in DCM (0.5 mL, 50%) for 2 h at ambient temperature. The cleavage cocktail was evaporated by a stream of nitrogen and oily residue was extracted into 1 mL of MeOH and analyzed by HPLC-UV-MS. Loading of resin was determined with the use of an external standard (Fmoc-Ala-OH, 0.5 mg/mL). Calculated loading was 0.40 mmol/g.

Further solid-phase synthesis of target compounds starting from resin **SM-2** was performed according to previously reported protocols [23].

4.1.4. Solution-Phase Synthesis of imidazo[4,5-*b*]pyridines

4.1.4.1. Reaction of 2,4-dichloro-3-nitropyridine with Boc-piperazine (**I-4**)

2,4-dichloro-3-nitropyridine (5 g, 26 mmol) and 1-Boc-piperazine (6.2 g, 30 mmol) were dissolved in DMSO (25 mL) and DIEA (5.2 mL, 30 mmol) was added. The reaction mixture was stirred at room temperature for 2 h. The reaction mixture was diluted with water (100 mL). The resulting suspension was filtered and washed with water. Dry crude product was suspended in *n*-hexane/toluene (10/1 v/v, 70 mL). The suspension was briefly boiled and filtered hot. The solid material was washed with a *n*-hexane/toluene (10/1 v/v) and *n*-hexane to give 7.69 g of product (yield 87%).

4.1.4.2. Reaction of I-4 with benzylamines or phenethylamines (I-5)

The corresponding amine (5.3 mmol) and 4-(*N*-Boc-piperazine)-2-chlor-3-nitro-pyridine (3.5 mmol) **I-1** were dissolved in DMSO (10 mL) and DIEA (6.4 mmol) was added. The reaction mixture was heated at 100°C for 48 h. After cooling, the reaction mixture was diluted with water (50 mL). The resulting mixture was extracted with EtOAc (2 x). The combined organic layers were washed with water (3 x), with brine (1 x) and concentrated *in vacuo*. The solid residue was suspended in methanol/water (2/1 v/v, 10 mL), washed with methanol/water (2/1 v/v, 5 mL) and water to give the final products in yields ranging from 70 to 90%.

4.1.4.3. Reduction of I-2 with sodium dithionate (I-6)

A solution of **I-5** (2.9 mmol) in DMF (24 mL) was heated to 80°C followed by addition of solution of Na₂S₂O₄ (7.9 mmol) and K₂CO₃ (7.9 mmol) in water (8 mL). The resulting mixture was heated at 80°C. After 1 h another portion of Na₂S₂O₄ (7.9 mmol) and K₂CO₃ (7.9 mmol) in water (8 mL) was added. The resulting mixture was heated at 80°C for 30 min. After cooling the reaction mixture, water (100 mL) and solution of ammonia 35 % (8 mL) were added. The resulting mixture was stirred at room temperature for 10 minutes. The suspension was filtered, washed with water and drier in air. Crude products were obtained in yields 60–90% and used in the next step without further purification.

4.1.4.4. Cyclization with aldehydes (I-7)

A solution of **I-6** (0.7 mmol) and aldehyde (2.2 mmol) in DMF (3 mL) was heated at 90°C for 48 h. After cooling, the reaction mixture was diluted with water (30 mL). The resulting mixture was extracted with EtOAc (2 x). The combined organic layers were washed with water (3 x), with brine (1 x) and concentrated *in vacuo*. The solid material was suspended in methanol/water (2/1 v/v, 5 mL), filtered, washed with methanol/water (2/1 v/v, 5 mL) and water to give final compounds in yields ranging from 70 to 80%.

4.1.4.5. Cleavage of Boc-protecting group

To a suspension of **I-7** (0.6 mol) in EtOH (1.9 mL), 5-10% HCl(g) (2.3 mL) in MeOH or EtOH was added. The resulting solution was stirred at room temperature for 2 days. The reaction mixture was concentrated to dryness. The residual material was co-evaporated with ether (2 x) and then suspended in ether. The suspension was filtrated and washed with ether and acetone to give the final compounds as white solids (yields 70-80%)

4.1.5. Characterization data for final compounds (**1-39**)

4.1.5.1. 3-Benzyl-7-(piperazin-1-yl)-3H-imidazo[4,5-c]pyridine acetate (**1**)

White solid, overall yield 45%; UHPLC-UV purity 99.0% (220 nm); C₁₉H₂₃N₅O₂, MW 353.43. ¹H NMR (500 MHz, DMSO-*d*₆) δ ppm: 3.27 (br. s., 4H), 4.41 (br. s., 4H), 5.69 (s, 2H), 6.78 (d, *J* = 7.0 Hz, 1H), 7.20–7.40 (m, 3H), 7.40–7.60 (m, 2H), 8.20 (d, *J* = 7.0 Hz, 1H), 8.64 (s, 1H), 9.79 (br. s., 2H). ¹³C NMR (125 MHz, DMSO-*d*₆) δ ppm: 43.0, 45.6, 48.6, 103.7, 124.9, 127.2, 129.6, 129.9, 138.4, 140.6, 170.6. HRMS (ESI-TOF): *m/z* calcd for C₁₇H₁₉N₅ [M+H]⁺ 294.1713, found 294.1715.

4.1.5.2. 3-(3-Chlorobenzyl)-7-(piperazin-1-yl)-3H-imidazo[4,5-c]pyridine acetate (**2**)

White solid, overall yield 40%; UHPLC-UV purity 98.6% (220 nm); C₁₉H₂₂ClN₅O₂, MW 387.87. ¹H NMR (500 MHz, DMSO-*d*₆) δ ppm: 3.31 (br. s., 4H), 4.25 (br. s., 4H), 5.88 (s, 2H), 6.78 (d, *J* = 6.9 Hz, 1H), 7.35–7.55 (m, 3H), 7.66 (s, 1H), 8.51 (d, *J* = 6.9 Hz, 1H), 8.88 (s, 1H), 9.55 (br. s., 2H). ¹³C NMR (125 MHz, DMSO-*d*₆) δ ppm: 43.6, 46.2, 47.8, 103.0, 124.6, 128.0, 128.4, 129.0, 131.5, 134.1, 139.9, 142.5. HRMS (ESI-TOF): *m/z* calcd for C₁₇H₁₈ClN₅ [M+H]⁺ 328.1323, found 328.1326.

4.1.5.3. 3-Benzyl-2-methyl-7-(piperazin-1-yl)-3H-imidazo[4,5-c]pyridine acetate (**3**)

White solid, overall yield 41%; UHPLC-UV purity 98.0% (220 nm); C₂₀H₂₅N₅O₂, MW 367.45. ¹H NMR (500 MHz, DMSO-*d*₆) δ ppm: 2.48 (s, 3H), 3.28 (br. s., 4H), 4.36 (br. s., 4H), 5.78 (s, 2H), 6.99 (d, *J* = 6.9 Hz, 1H), 7.18 (d, *J* = 6.9 Hz, 2H), 7.25–7.33 (m, 1H), 7.31–7.38 (m, 2H), 8.18 (d, *J* = 6.9 Hz, 1H), 9.93 (br. s., 2H). ¹³C NMR (125 MHz, DMSO-*d*₆) δ ppm: 14.3, 42.6, 45.2, 47.6, 127.5, 128.6, 129.9, 135.1, 150.0, 173.5. HRMS (ESI-TOF): *m/z* calcd for C₁₈H₂₁N₅ [M+H]⁺ 308.1870, found 308.1872.

4.1.5.4. 1-(3-Chlorobenzyl)-2-methyl-4-(piperazin-1-yl)-1H-imidazo[4,5-c]pyridine acetate (**4**)

Pale yellow solid, overall yield 40%; UHPLC-UV purity 98.8% (220 nm); $C_{20}H_{24}ClN_5O_2$, MW 401.90. 1H NMR (500 MHz, DMSO- d_6) δ ppm: 1.77 (s, 3H), 2.43 (s, 3H), 2.82 (br. s., 4H), 3.94–3.99 (m, 4H), 5.40 (s, 2H), 6.82 (d, $J = 5.7$ Hz, 1H), 6.94–6.98 (m, 1H), 7.15 (s, 1H), 7.30–7.33 (m, 2H), 7.73 (d, $J = 5.7$ Hz, 1H). ^{13}C NMR (125 MHz, DMSO- d_6) δ ppm: 13.9, 23.1, 45.6, 46.3, 46.9, 98.0, 125.8, 127.0, 128.1, 131.3, 133.9, 139.8, 140.0, 141.8, 149.0, 151.2, 173.5. HRMS (ESI-TOF): m/z calcd for $C_{18}H_{20}ClN_5$ $[M+H]^+$ 342.1480, found 342.1484.

4.1.5.5. 3-(3-Chlorobenzyl)-2-isopropyl-7-(piperazin-1-yl)-3H-imidazo[4,5-b]pyridine acetate (5)

Pale yellow solid, overall yield 39%; UHPLC-UV purity 99.4% (220 nm); $C_{22}H_{28}ClN_5O_2$, MW 429.95. 1H NMR (500 MHz, DMSO- d_6) δ ppm: 1.17 (d, $J = 6.9$ Hz, 6H), 1.85 (s, 3H), 2.86 (br. s., 4H), 3.18 (dt, $J = 13.8, 6.9$ Hz, 1H), 3.97–4.03 (m, 4H), 5.45 (s, 2H), 6.80 (d, $J = 5.7$ Hz, 1H), 6.89 (t, $J = 3.7$ Hz, 1H), 7.12 (s, 1H), 7.28–7.33 (m, 2H), 7.73 (d, $J = 5.7$ Hz, 1H). ^{13}C NMR (125 MHz, DMSO- d_6) δ ppm: 22.2, 26.0, 45.6, 45.9, 46.9, 98.2, 125.4, 126.8, 127.2, 128.1, 131.3, 133.9, 140.0, 140.1, 141.6, 151.3, 156.9, 172.8. HRMS (ESI-TOF): m/z calcd for $C_{20}H_{24}ClN_5$ $[M+H]^+$ 370.1793, found 370.1794.

4.1.5.6. 3-Benzyl-7-(piperazin-1-yl)-3H-imidazo[4,5-b]pyridine hydrochloride (6)

White solid, overall yield 35%; UHPLC-UV purity 98.9% (220 nm); $C_{17}H_{20}ClN_5$, MW 329.83. 1H NMR (500 MHz, DMSO- d_6) δ ppm: 3.25 (br. s., 4H), 4.39 (br. s., 4H), 5.64 (s, 2H), 6.91 (d, $J = 7.0$ Hz, 1H), 7.25–7.34 (m, 3H), 7.36–7.40 (m, 2H), 8.15 (d, $J = 6.9$ Hz, 1H), 8.54 (s, 1H), 9.59 (br. s., 2H). ^{13}C NMR (125 MHz, DMSO- d_6) δ ppm: 42.8, 45.1, 48.0, 102.6, 123.9, 128.1, 128.7, 129.4, 136.5, 141.5. HRMS (ESI-TOF): m/z calcd for $C_{17}H_{19}N_5$ $[M+H]^+$ 294.1713, found 294.1715.

4.1.5.7. 3-(3-Chlorobenzyl)-7-(piperazin-1-yl)-3H-imidazo[4,5-b]pyridine hydrochloride (7)

White solid, overall yield 35%; UHPLC-UV purity 98.9% (220 nm); $C_{17}H_{19}Cl_2N_5$, MW 364.27. 1H NMR (500 MHz, DMSO- d_6) δ ppm: 3.25 (br. s., 4H), 4.38 (br. s., 4H), 5.64 (s, 2H), 6.90 (d, $J = 6.9$ Hz, 1H), 7.29–7.40 (m, 3H), 7.52 (s, 1H), 8.14 (d, $J = 6.8$ Hz, 1H), 8.56 (s, 1H), 9.55 (br. s., 2H). ^{13}C NMR (125 MHz, DMSO- d_6) δ ppm: 42.9, 45.1, 47.3, 102.7, 124.0, 126.9, 128.2, 128.7, 131.3, 133.9, 138.9, 141.5. HRMS (ESI-TOF): m/z calcd for $C_{17}H_{18}ClN_5$ $[M+H]^+$ 328.1323, found 328.1326.

4.1.5.8. 3-Benzyl-2-methyl-7-(piperazin-1-yl)-3H-imidazo[4,5-b]pyridine hydrochloride (8)

White solid, overall yield 32%; UHPLC-UV purity 99.1% (220 nm); $C_{18}H_{22}ClN_5$, MW 343.86. 1H NMR (500 MHz, DMSO- d_6) δ ppm: 2.47 (s, 3H), 3.26 (br. s., 4H), 4.38 (br. s., 4H), 5.74 (s, 2H),

6.96 (d, $J = 6.9$ Hz, 1H), 7.16 (d, $J = 6.9$ Hz, 2H), 7.25–7.30 (m, 1H), 7.29–7.35 (m, 2H), 8.12 (d, $J = 6.9$ Hz, 1H), 9.83 (br. s., 2H). ^{13}C NMR (125 MHz, DMSO- d_6) δ ppm: 14.2, 42.8, 45.2, 47.3, 127.4, 128.5, 129.5, 135.8, 150.0. HRMS (ESI-TOF): m/z calcd for $\text{C}_{18}\text{H}_{21}\text{N}_5$ $[\text{M}+\text{H}]^+$ 308.1870, found 308.1872.

4.1.5.9. 3-(2-Chlorobenzyl)-2-methyl-7-(piperazin-1-yl)-3H-imidazo[4,5-b]pyridine hydrochloride (9)

White solid, overall yield 39%; UHPLC-UV purity 98.9% (220 nm); $\text{C}_{18}\text{H}_{21}\text{Cl}_2\text{N}_5$, MW 378.30. ^1H NMR (500 MHz, DMSO- d_6) δ ppm: 2.39 (s, 3H), 3.27 (br. s., 4H), 4.42 (br. s., 4H), 5.80 (s, 2H), 6.60 (d, $J = 6.9$ Hz, 1H), 7.00 (d, $J = 6.9$ Hz, 1H), 7.20–7.27 (m, 1H), 7.34 (td, $J = 7.7, 1.7$ Hz, 1H), 7.53 (dd, $J = 8.0, 1.2$ Hz, 1H), 8.12 (d, $J = 7.5$ Hz, 1H). ^{13}C NMR (125 MHz, DMSO- d_6) δ ppm: 14.0, 42.8, 45.2, 45.9, 100.0, 103.4, 127.6, 128.4, 130.2, 130.4, 132.2, 132.9, 149.1, 150.1. HRMS (ESI-TOF): m/z calcd for $\text{C}_{18}\text{H}_{20}\text{ClN}_5$ $[\text{M}+\text{H}]^+$ 342.1480, found 342.1482.

4.1.5.10. 3-(2-Methoxybenzyl)-2-methyl-7-(piperazin-1-yl)-3H-imidazo[4,5-b]pyridine acetate (10)

White solid, overall yield 36%; UHPLC-UV purity 99.3% (220 nm); $\text{C}_{21}\text{H}_{27}\text{N}_5\text{O}_3$, MW 397.48. ^1H NMR (400 MHz, DMSO- d_6) δ ppm: 1.77 (s, 3H), 2.37 (s, 3H), 2.85 (br. s., 4H), 3.74–3.80 (m, 4H), 3.84 (s, 3H), 5.29 (s, 2H), 6.41–6.47 (m, 2H), 6.75 (d, $J = 1.4$ Hz, 1H), 7.01 (d, $J = 8.2$ Hz, 1H), 7.16–7.24 (m, 1H), 7.83 (dd, $J = 5.7, 1.2$ Hz, 1H). ^{13}C NMR (125 MHz, DMSO- d_6) δ ppm: 14.2, 23.3, 40.9, 45.5, 48.4, 55.9, 102.4, 111.3, 120.9, 123.7, 125.2, 127.1, 129.1, 144.4, 147.3, 148.3, 149.7, 156.7, 173.8. HRMS (ESI-TOF): m/z calcd for $\text{C}_{19}\text{H}_{23}\text{N}_5\text{O}$ $[\text{M}+\text{H}]^+$ 338.1975, found 338.1976.

4.1.5.11. 3-(3-Methylbenzyl)-2-methyl-7-(piperazin-1-yl)-3H-imidazo[4,5-b]pyridine hydrochloride (11)

White solid, overall yield 32%; UHPLC-UV purity 98.5% (220 nm); $\text{C}_{19}\text{H}_{24}\text{ClN}_5$, MW 357.89. ^1H NMR (500 MHz, DMSO- d_6) δ ppm: 2.22 (s, 3H), 2.46 (br. s., 3H), 3.26 (br. s., 4H), 4.37 (br. s., 4H), 5.67 (s, 2H), 6.90 (d, $J = 8.0$ Hz, 1H), 6.96 (d, $J = 7.5$ Hz, 1H), 7.00 (s, 1H), 7.09 (d, $J = 8.0$ Hz, 1H), 7.14–7.24 (m, 1H), 8.13 (d, $J = 6.9$ Hz, 1H), 9.75 (br. s., 2H). ^{13}C NMR (125 MHz, DMSO- d_6) δ ppm: 14.2, 21.5, 42.9, 45.2, 47.2, 124.4, 127.9, 129.4, 135.7, 138.8, 148.9, 150.0. HRMS (ESI-TOF): m/z calcd for $\text{C}_{19}\text{H}_{23}\text{N}_5$ $[\text{M}+\text{H}]^+$ 322.2026, found 322.2024.

4.1.5.12. 3-(3-Chlorobenzyl)-2-methyl-7-(piperazin-1-yl)-3H-imidazo[4,5-b]pyridine acetate (12)

Pale yellow solid, overall yield 35%; UHPLC-UV purity 99.3% (220 nm); $C_{20}H_{24}ClN_5O_2$, MW 401.90. 1H NMR (500 MHz, DMSO- d_6) δ ppm: 1.84 (s, 3H), 2.39 (s, 3H), 2.80–2.85 (m, 4H), 3.73–3.78 (m, 4H), 5.38 (s, 2H), 6.47 (d, $J = 5.7$ Hz, 1H), 7.03–7.07 (m, 1H), 7.21 (s, 1H), 7.28–7.33 (m, 2H), 7.89 (d, $J = 5.7$ Hz, 1H). ^{13}C NMR (125 MHz, DMSO- d_6) δ ppm: 14.4, 22.1, 44.6, 45.8, 48.6, 102.5, 123.5, 126.0, 127.2, 128.0, 131.2, 133.8, 140.3, 144.6, 147.4, 147.9, 149.5, 172.9. HRMS (ESI-TOF): m/z calcd for $C_{18}H_{20}ClN_5$ $[M+H]^+$ 342.1480, found 342.1482.

4.1.5.13.3-[3-(Trifluoromethyl)benzyl]-2-methyl-7-(piperazin-1-yl)-3H-imidazo[4,5-b]pyridine trifluoroacetate (**13**)

White solid, overall yield 41%; UHPLC-UV purity 99.0% (220 nm); $C_{21}H_{21}F_6N_5O_2$, MW 489.42. 1H NMR (500 MHz, DMSO- d_6) δ ppm: 2.66 (s, 3H), 3.55 (br. s., 4H), 4.88 (br. s., 4H), 5.78 (s, 2H), 6.99 (d, $J = 7.5$ Hz, 1H), 7.30–7.40 (m, 2H), 7.45 (dd, $J = 8.5, 5.5$ Hz, 2H), 8.20 (d, $J = 6.9$ Hz, 1H), 9.99 (br. s., 2H). ^{13}C NMR (125 MHz, DMSO- d_6) δ ppm: 15.2, 43.6, 45.9, 47.5, 117.3, 118.3, 131.8, 150.8, 163.2, 164.3, 166.7, 172.1, 173.0. HRMS (ESI-TOF): m/z calcd for $C_{19}H_{20}F_3N_5$ $[M+H]^+$ 376.1744, found 376.1745.

4.1.5.14.3-(4-Fluorobenzyl)-2-methyl-7-(piperazin-1-yl)-3H-imidazo[4,5-b]pyridine hydrochloride (**14**)

White solid, overall yield 36%; UHPLC-UV purity 99.0% (220 nm); $C_{18}H_{21}ClFN_5$, MW 361.85. 1H NMR (500 MHz, DMSO- d_6) δ ppm: 2.47 (s, 3H), 3.25 (br. s., 4H), 4.35 (br. s., 4H), 5.69 (s, 2H), 6.93 (d, $J = 7.5$ Hz, 1H), 7.10–7.20 (m, 2H), 7.26 (dd, $J = 8.6, 5.7$ Hz, 2H), 8.11 (d, $J = 6.9$ Hz, 1H), 9.78 (br. s., 2H). ^{13}C NMR (125 MHz, DMSO- d_6) δ ppm: 14.2, 42.8, 45.1, 46.5, 116.2, 116.4, 129.8, 149.8, 161.3, 163.2, 164.5. (ESI-TOF): m/z calcd for $C_{18}H_{20}FN_5$ $[M+H]^+$ 326.1776, found 326.1777.

4.1.5.15.3-Benzyl-2-ethyl-7-(piperazin-1-yl)-3H-imidazo[4,5-b]pyridine hydrochloride (**15**)

White solid, overall yield 40%; UHPLC-UV purity 98.0% (220 nm); $C_{19}H_{24}ClN_5$, MW 357.89. 1H NMR (500 MHz, DMSO- d_6) δ ppm: 1.15 (t, $J = 7.5$ Hz, 3H), 2.75 (q, $J = 7.5$ Hz, 2H), 3.27 (br. s., 4H), 4.39 (br. s., 4H), 5.67 (s, 2H), 6.92 (d, $J = 7.5$ Hz, 1H), 7.07–7.14 (m, 2H), 7.25–7.29 (m, 1H), 7.29–7.35 (m, 2H), 8.11 (d, $J = 7.5$ Hz, 1H), 9.59 (br. s., 2H). ^{13}C NMR (125 MHz, DMSO- d_6) δ ppm: 11.5, 20.6, 42.9, 45.1, 46.7, 100.0, 103.0, 127.2, 128.5, 129.5, 136.2, 153.8. HRMS (ESI-TOF): m/z calcd for $C_{19}H_{23}N_5$ $[M+H]^+$ 322.2026, found 322.2028.

4.1.5.16. 3-(2-Chlorobenzyl)-2-ethyl-7-(piperazin-1-yl)-3H-imidazo[4,5-b]pyridine hydrochloride
(16)

Yellow solid, overall yield 38%; UHPLC-UV purity 99.1% (220 nm); $C_{19}H_{23}Cl_2N_5$, MW 392.33. 1H NMR (500 MHz, DMSO- d_6) δ ppm 1.16 (t, $J = 7.5$ Hz, 3H), 2.69 (q, $J = 7.5$ Hz, 2H), 2.81–2.88 (m, 4H), 3.76–3.83 (m, 4H), 5.43 (s, 2H), 6.39 (d, $J = 7.5$ Hz, 1H), 6.47 (d, $J = 5.7$ Hz, 1H), 7.16 (t, $J = 7.5$ Hz, 1H), 7.26 (t, $J = 7.7$ Hz, 1H), 7.49 (d, $J = 8.0$ Hz, 1H), 7.83 (d, $J = 5.7$ Hz, 1H). ^{13}C NMR (125 MHz, DMSO- d_6) δ ppm 11.9, 20.8, 22.5, 42.9, 45.8, 102.6, 123.6, 127.5, 128.2, 129.6, 130.0, 131.8, 135.0, 144.7, 147.6, 149.6, 152.2, 173.2. HRMS (ESI-TOF): m/z calcd for $C_{19}H_{22}ClN_5$ $[M+H]^+$ 356.1636, found 356.1638.

4.1.5.17. 3-(3-Fluorobenzyl)-2-ethyl-7-(piperazin-1-yl)-3H-imidazo[4,5-b]pyridine dihydrochloride
(17)

White solid, overall yield 42 %, UHPLC-UV purity 99.2% (220 nm); $C_{19}H_{24}Cl_2FN_5 \cdot H_2O$, MW 430.35. 1H NMR (500 MHz, DMSO- d_6) δ ppm: 1.20 (t, $J = 7.3$ Hz, 3H), 2.79 (q, $J = 7.3$ Hz, 2H), 3.29 (br. s., 4H), 4.45 (br. s., 4H), 5.79 (s, 2H), 6.93–7.00 (m, 2H), 7.08 (dd, $J = 2.1, 9.9$ Hz, 1H), 7.15 (dt, $J = 2.3, 8.4$ Hz, 1H), 7.40 (dt, $J = 6.0, 7.9$ Hz, 1H), 8.14 (d, $J = 7.3$ Hz, 1H), 9.86 (br. s., 2H). ^{13}C NMR (125 MHz, DMSO- d_6) δ ppm: 10.9, 20.0, 42.3, 44.6, 45.9, 102.6, 113.9 (d, $J = 22.0$ Hz), 114.8 (d, $J = 21.0$ Hz), 122.2 (d, $J = 2.9$ Hz), 122.7, 131.0 (d, $J = 8.6$ Hz), 136.1, 138.4 (d, $J = 7.7$ Hz), 141.9, 148.4, 153.3, 162.3 (d, $J = 245.0$ Hz). HRMS (ESI-TOF): m/z calcd for $C_{29}H_{22}FN_5$ $[M+H]^+$ 340.1932, found 340.1935. Anal. calcd for $C_{19}H_{26}Cl_2FN_5O$: C: 53.03, H: 6.09, N: 16.27; Found C: 53.23, H: 5.69, N: 16.26.

4.1.5.18. 3-(3-Chlorobenzyl)-2-ethyl-7-(piperazin-1-yl)-3H-imidazo[4,5-b]pyridine hydrochloride
(18)

White solid, overall yield 41%; UHPLC-UV purity 99.5% (220 nm); $C_{19}H_{23}Cl_2N_5$, MW 392.33. 1H NMR (500 MHz, DMSO- d_6) δ ppm: 1.16 (t, $J = 7.5$ Hz, 3H), 2.75 (q, $J = 7.5$ Hz, 2H), 3.26 (br. s., 4H), 4.43 (br. s., 4H), 5.77 (s, 2H), 6.95 (d, $J = 6.9$ Hz, 1H), 7.04 (t, $J = 3.7$ Hz, 1H), 7.29 (s, 1H), 7.31–7.42 (m, 2H), 8.11 (d, $J = 6.9$ Hz, 1H), 9.87 (br. s., 2H). ^{13}C NMR (125 MHz, DMSO- d_6) δ ppm: 11.5, 20.6, 42.8, 45.2, 46.5, 103.1, 125.9, 127.3, 128.5, 131.4, 134.0, 138.6, 149.0, 153.8. HRMS (ESI-TOF): m/z calcd for $C_{19}H_{22}ClN_5$ $[M+H]^+$ 356.1736, found 356.1739.

4.1.5.19. 3-(2,5-Difluorobenzyl)-2-ethyl-7-(piperazin-1-yl)-3H-imidazo[4,5-b]pyridine acetate (19)

White solid, overall yield 35%; UHPLC-UV purity 98.8% (220 nm); $C_{21}H_{25}F_2N_5O_2$, MW 417.46. 1H NMR (500 MHz, DMSO- d_6) δ ppm: 1.16 (t, $J = 7.5$ Hz, 3H), 1.84 (s, 3H), 2.75 (q, $J = 7.5$ Hz, 2H), 3.25 (br. s., 4H), 4.39 (br. s., 4H), 5.75 (br. s., 2H), 6.91 (d, $J = 4.01$ Hz, 1H), 7.17–7.25 (m, 1H), 7.26–7.32 (m, 1H), 7.34 (d, $J = 5.7$ Hz, 1H), 8.09 (d, $J = 6.9$ Hz, 1H). ^{13}C NMR (125 MHz, DMSO- d_6) δ ppm: 11.4, 20.5, 23.3, 41.8, 42.8, 45.1, 103.1, 115.8, 116.0, 117.0, 117.9, 118.1, 122.7, 148.7, 153.7, 155.6, 157.6, 157.7, 159.6, 173.6. HRMS (ESI-TOF): m/z calcd for $C_{19}H_{21}F_2N_5$ $[M+H]^+$ 358.1838, found 358.1840.

4.1.5.20.3-(3,4-Difluorobenzyl)-2-ethyl-7-(piperazin-1-yl)-3H-imidazo[4,5-b]pyridine acetate (20)

White solid, overall yield 35%; UHPLC-UV purity 98.9% (220 nm); $C_{21}H_{25}F_2N_5O_2$, MW 417.46. 1H NMR (500 MHz, DMSO- d_6) δ ppm: 1.15 (t, $J = 7.7$ Hz, 3H), 1.85 (s, 3H), 2.73 (q, $J = 7.5$ Hz, 2H), 2.80–2.86 (m, 4H), 3.72–3.81 (m, 4H), 5.36 (s, 2H), 6.47 (d, $J = 5.7$ Hz, 1H), 6.87–6.94 (m, 1H), 7.24 (dd, $J = 10.9, 8.6$ Hz, 1H), 7.29–7.36 (m, 1H), 7.89 (d, $J = 5.7$ Hz, 1H). ^{13}C NMR (125 MHz, DMSO- d_6) δ ppm: 12.0, 20.8, 22.1, 43.9, 45.7, 48.6, 102.5, 116.6, 118.3, 118.4, 123.5, 124.2, 135.8, 144.7, 147.5, 148.8, 149.6, 150.3, 150.8, 152.0, 173.0. HRMS (ESI-TOF): m/z calcd for $C_{19}H_{21}F_2N_5$ $[M+H]^+$ 358.1838, found 358.1841.

4.1.5.21.3-(2-Fluorobenzyl)-2-isopropyl-7-(piperazin-1-yl)-3H-imidazo[4,5-b]pyridine hydrochloride (21)

White solid, overall yield 30%; UHPLC-UV purity 99.0% (220 nm); $C_{20}H_{25}ClFN_5$, MW 389.90. 1H NMR (500 MHz, DMSO- d_6) δ ppm: 1.10 (d, $J = 6.9$ Hz, 6H), 3.08–3.19 (m, 1H), 3.27 (br. s., 4H), 4.44 (br. s., 4H), 5.82 (s, 2H), 5.66–5.92 (m, 2H), 6.88–7.02 (m, 2H), 7.13 (t, $J = 7.5$ Hz, 1H), 7.18–7.27 (m, 1H), 7.30–7.41 (m, 1H), 8.12 (d, $J = 6.9$ Hz, 1H), 9.82 (br. s., 2H). ^{13}C NMR (125 MHz, DMSO- d_6) δ ppm: 21.8, 26.3, 42.2, 42.2, 42.8, 45.1, 102.9, 116.12, 116.4, 122.8, 123.3, 123.4, 125.4, 125.4, 129.0, 129.1, 130.8, 130.9, 149.1, 157.4, 159.4, 161.4. HRMS (ESI-TOF): m/z calcd for $C_{20}H_{24}FN_5$ $[M+H]^+$ 354.2089, found 354.2090.

4.1.5.22.3-(3-Fluorobenzyl)-2-isopropyl-7-(piperazin-1-yl)-3H-imidazo[4,5-b]pyridine hydrochloride (22)

White solid, overall yield 34%, UHPLC-UV purity 99.4% (220 nm); $C_{20}H_{25}ClFN_5$, MW 389.90. 1H NMR (500 MHz, DMSO- d_6) δ ppm: 1.17 (d, $J = 6.5$ Hz, 6H), 3.12–3.24 (m, 1H), 3.30 (br. s., 4H), 4.47 (br. s., 4H), 5.83 (s, 2H), 6.91 (d, $J = 7.5$ Hz, 1H), 6.97 (d, $J = 7.0$ Hz, 1H), 7.06 (d, $J = 9.9$ Hz, 1H), 7.10–7.20 (m, 1H), 7.33–7.46 (m, $J = 7.1, 7.1, 7.1$ Hz, 1H), 8.13 (d, $J = 6.7$ Hz, 1H), 9.89 (br. s., 2H). ^{13}C NMR (125 MHz, DMSO- d_6) δ ppm: 21.3, 25.8, 42.3, 44.6, 45.9, 102.5, 113.7 (d,

$J = 21.0$ Hz), 114.8 (d, $J = 21.0$ Hz), 122.4, 122.5, 131.0 (d, $J = 10.1$ Hz), 135.9, 138.7 (d, $J = 7.7$ Hz), 141.5, 148.6, 156.8, 162.2 (d, $J = 246$ Hz). HRMS (ESI-TOF): m/z calcd for $C_{20}H_{24}FN_5$ $[M+H]^+$ 354.2089, found 354.2093.

4.1.5.23. 3-(3-Chlorobenzyl)-2-isopropyl-7-(piperazin-1-yl)-3H-imidazo[4,5-b]pyridine
hydrochloride (**23**)

White solid, overall yield 33%, UHPLC-UV purity 98.9% (220 nm); $C_{20}H_{25}Cl_2N_5$, MW 406.36. 1H NMR (400 MHz, DMSO- d_6) δ ppm: 1.17 (d, $J = 6.7$ Hz, 6H), 3.19 (td, $J = 6.7, 13.5$ Hz, 1H), 3.30 (br. s., 4H), 4.47 (br. s., 4H), 5.83 (s, 2H), 6.97 (d, $J = 7.3$ Hz, 1H), 7.00–7.05 (m, 1H), 7.31 (s, 1H), 7.35–7.40 (m, 2H), 8.13 (d, $J = 6.7$ Hz, 1H), 9.90 (br. s., 2H). ^{13}C NMR (101 MHz, DMSO- d_6) δ ppm: 21.5, 26.0, 42.5, 44.8, 46.0, 102.7, 122.6, 125.4, 126.9, 128.1, 131.0, 133.6, 136.2, 138.6, 141.6, 148.8, 157.0. HRMS (ESI-TOF): m/z calcd for $C_{20}H_{24}ClN_5$ $[M+H]^+$ 370.1793, found 370.1794.

4.1.5.24. 3-(3-Methoxybenzyl)-2-isopropyl-7-(piperazin-1-yl)-3H-imidazo[4,5-b]pyridine acetate
(**24**)

White solid, overall yield 38%; UHPLC-UV purity 99.0% (220 nm); $C_{23}H_{31}N_5O_3$, MW 425.53. 1H NMR (400 MHz, DMSO- d_6) δ ppm: 1.14 (d, $J = 6.6$ Hz, 6H), 1.83 (s, 3H), 2.86 (br. s., 4H), 3.07–3.16 (m, 1H), 3.64 (s, 3H), 3.78 (d, $J = 4.1$ Hz, 4H), 5.38 (s, 2H), 6.47 (d, $J = 5.7$ Hz, 1H), 6.57 (d, $J = 7.8$ Hz, 1H), 6.67–6.71 (m, 1H), 6.78 (dd, $J = 8.2, 2.5$ Hz, 1H), 7.17 (t, $J = 8.0$ Hz, 1H), 7.89 (d, $J = 5.7$ Hz, 1H). ^{13}C NMR (125 MHz, DMSO- d_6) δ ppm 22.0, 26.5, 31.2, 44.7, 45.5, 48.5, 55.5, 102.5, 112.9, 113.2, 119.1, 126.6, 130.3, 139.8, 155.6, 147.5, 149.5, 155.9, 159.9, 173.2. HRMS (ESI-TOF): m/z calcd for $C_{21}H_{27}N_5O$ $[M+H]^+$ 366.2288, found 366.2290.

4.1.5.25. 3-(4-Fluorobenzyl)-2-isopropyl-7-(piperazin-1-yl)-3H-imidazo[4,5-b]pyridine
hydrochloride (**25**)

White solid, overall yield 32%; UHPLC-UV purity 99.3% (220 nm); $C_{20}H_{25}ClFN_5$, MW 389.90. 1H NMR (500 MHz, DMSO- d_6) δ ppm: 1.13 (d, $J = 6.9$ Hz, 6H), 3.12–3.21 (m, 1H), 3.26 (br. s., 4H), 4.43 (br. s., 4H), 5.76 (s, 2H), 6.94 (d, $J = 6.9$ Hz, 1H), 7.09–7.23 (m, 4H), 8.10 (d, $J = 6.9$ Hz, 1H), 9.83 (br. s., 2H). ^{13}C NMR (125 MHz, DMSO- d_6) δ ppm: 21.8, 26.4, 42.8, 45.1, 46.3, 102.9, 116.2, 116.3, 122.9, 129.4, 129.5, 132.7, 157.4, 161.2, 163.2, 170.2, 171.1. HRMS (ESI-TOF): m/z calcd for $C_{20}H_{24}FN_5$ $[M+H]^+$ 354.2089, found 354.2092.

4.1.5.26. 3-(4-Chlorobenzyl)-2-isopropyl-7-(piperazin-1-yl)-3H-imidazo[4,5-b]pyridine
hydrochloride (**26**)

White solid, overall yield 38%; UHPLC-UV purity 99.0% (220 nm); C₂₀H₂₅Cl₂N₅, MW 406.36. ¹H NMR (500 MHz, DMSO-*d*₆) δ ppm: 1.13 (d, *J* = 6.3 Hz, 6H), 3.04–3.21 (m, 1H), 3.27 (br. s., 4H), 4.42 (br. s., 4H), 5.76 (s, 2H), 6.93 (d, *J* = 6.9 Hz, 1H), 7.12 (d, *J* = 8.0 Hz, 2H), 7.32–7.44 (m, 2H), 8.03–8.15 (m, 1H), 9.77 (br. s., 2H). ¹³C NMR (125 MHz, DMSO-*d*₆) δ ppm: 21.8, 26.3, 42.8, 45.1, 46.2, 103.0, 122.9, 129.0, 129.4, 133.0, 135.5, 157.3. HRMS (ESI-TOF): *m/z* calcd for C₂₀H₂₄ClN₅ [M+H]⁺ 370.1793, found 370.1796.

4.1.5.27. 3-(2-Chlorobenzyl)-2-(pentan-3-yl)-7-(piperazin-1-yl)-3H-imidazo[4,5-b]pyridine acetate
(**27**)

Yellow solid, overall yield 35%; UHPLC-UV purity 99.2% (220 nm); C₂₄H₃₂ClN₅O₂, MW 458.00. ¹H NMR (500 MHz, DMSO-*d*₆) δ ppm: 0.60–0.65 (m, 6H), 1.51–1.60 (m, 2H), 1.61–1.71 (m, 2H), 1.82 (s, 3H), 2.62 (s, 1H), 2.90 (br. s., 4H), 3.84 (d, *J* = 3.4 Hz, 4H), 5.46 (s, 2H), 6.50 (d, *J* = 5.7 Hz, 2H), 7.14 (td, *J* = 7.5, 1.2 Hz, 1H), 7.25 (td, *J* = 7.7, 1.7 Hz, 1H), 7.46–7.50 (m, 1H), 7.87 (d, *J* = 5.7 Hz, 1H). ¹³C NMR (125 MHz, DMSO-*d*₆) δ ppm: 12.1, 22.5, 27.1, 42.5, 45.1, 48.1, 102.7, 123.9, 128.0, 128.2, 129.7, 129.9, 131.8, 135.2, 144.6, 147.3, 149.3, 154.1, 173.3. HRMS (ESI-TOF): *m/z* calcd for C₂₂H₂₈ClN₅ [M+H]⁺ 398.2106, found 398.2109.

4.1.5.28. 3-(3-Chlorobenzyl)-2-(pentan-3-yl)-7-(piperazin-1-yl)-3H-imidazo[4,5-b]pyridine
hydrochloride (**28**)

Yellow solid, overall yield 34%; UHPLC-UV purity 98.3% (220 nm); C₂₄H₃₂ClN₅O₂, MW 458.00. ¹H NMR (500 MHz, DMSO-*d*₆) δ ppm: 0.61 (t, *J* = 7.5 Hz, 6H), 0.99 (d, *J* = 6.3 Hz, 1H), 1.49–1.67 (m, 4H), 2.74–2.83 (m, 1H), 3.26 (br. s., 4H), 3.74 (td, *J* = 12.3, 6.3 Hz, 1H), 4.44 (br. s., 4H), 5.74–5.83 (m, 2H), 6.95 (d, *J* = 6.9 Hz, 1H), 7.01–7.09 (m, 1H), 7.30 (s, 1H), 7.31–7.37 (m, 2H), 8.12 (d, *J* = 7.5 Hz, 1H), 9.81 (br. s., 2H). ¹³C NMR (125 MHz, DMSO-*d*₆) δ ppm: 11.9, 26.0, 27.2, 42.8, 45.1, 46.3, 103.0, 123.2, 126.1, 127.4, 128.5, 131.2, 133.9, 139.0, 149.1, 155.7. HRMS (ESI-TOF): *m/z* calcd for C₂₂H₂₈ClN₅ [M+H]⁺ 398.2106, found 398.2108.

4.1.5.29. 3-(3-Methylbenzyl)-2-(pentan-3-yl)-7-(piperazin-1-yl)-3H-imidazo[4,5-b]pyridine
hydrochloride (**29**)

White solid, overall yield 40%; UHPLC-UV purity 98.8% (220 nm); C₂₃H₃₂ClN₅, MW 413.99. ¹H NMR (500 MHz, DMSO-*d*₆) δ ppm: 0.60 (t, *J* = 7.5 Hz, 6H), 1.43–1.69 (m, 4H), 2.21 (s, 3H), 2.72–

2.84 (m, 1H), 3.27 (br. s., 4H), 4.45 (d, $J = 1.7$ Hz, 4H), 5.71 (s, 2H), 6.87 (d, $J = 7.5$ Hz, 1H), 6.92–7.00 (m, 2H), 7.08 (d, $J = 7.5$ Hz, 1H), 7.12–7.23 (m, 1H), 8.12 (d, $J = 6.9$ Hz, 1H), 9.82 (br. s., 2H). ^{13}C NMR (125 MHz, DMSO- d_6) δ ppm: 11.8, 21.5, 27.1, 42.8, 45.1, 47.0, 102.9, 124.4, 127.9, 129.1, 129.2, 136.3, 138.5, 155.9. HRMS (ESI-TOF): m/z calcd for $\text{C}_{23}\text{H}_{31}\text{N}_5$ $[\text{M}+\text{H}]^+$ 378.2652, found 378.2655.

4.1.5.30.3-(3-Methylbenzyl)-2-neopentyl-7-(piperazin-1-yl)-3H-imidazo[4,5-b]pyridine
hydrochloride (**30**)

White solid, overall yield 38%; UHPLC-UV purity 99.2% (220 nm); $\text{C}_{23}\text{H}_{32}\text{ClN}_5$, MW 413.99. ^1H NMR (500 MHz, DMSO- d_6) δ ppm: 0.94 (s, 9H), 2.21 (s, 3H), 2.67 (s, 2H), 3.27 (br. s., 4H), 4.46 (br. s., 4H), 5.72 (s, 2H), 6.82 (d, $J = 7.5$ Hz, 1H), 6.89–7.00 (m, 2H), 7.07 (d, $J = 7.5$ Hz, 1H), 7.13–7.22 (m, 1H), 8.10 (d, $J = 6.9$ Hz, 1H), 9.86 (br. s., 2H). ^{13}C NMR (125 MHz, DMSO- d_6) δ ppm: 21.5, 29.7, 32.8, 42.8, 45.1, 47.1, 102.9, 122.9, 124.2, 127.8, 129.1, 129.3, 136.1, 138.6, 151.1. HRMS (ESI-TOF): m/z calcd for $\text{C}_{23}\text{H}_{31}\text{N}_5$ $[\text{M}+\text{H}]^+$ 378.2652, found 378.2654.

4.1.5.31.3-(3-Methoxybenzyl)-2-neopentyl-7-(piperazin-1-yl)-3H-imidazo[4,5-b]pyridine
acetate (**31**)

White solid, overall yield 42%; UHPLC-UV purity 98.9% (220 nm); $\text{C}_{25}\text{H}_{35}\text{N}_5\text{O}_3$, MW 453.59. ^1H NMR (500 MHz, DMSO- d_6) δ ppm: 0.94 (s, 9H), 1.80 (s, 3H), 2.61 (s, 2H), 2.84 (br. s., 4H), 3.64 (s, 3H), 3.80 (br. s., 4H), 5.38 (s, 2H), 6.46 (d, $J = 5.7$ Hz, 1H), 6.57 (d, $J = 8.0$ Hz, 1H), 6.67 (s, 1H), 6.77 (dd, $J = 8.3, 2.6$ Hz, 1H), 7.16 (t, $J = 7.7$ Hz, 1H), 7.88 (d, $J = 5.7$ Hz, 1H). ^{13}C NMR (125 MHz, DMSO- d_6) δ ppm: 22.8, 29.9, 32.6, 45.0, 45.7, 48.6, 55.5, 102.4, 112.9, 113.3, 119.2, 123.7, 130.3, 139.7, 144.6, 147.3, 149.2, 149.4, 159.9, 172.8. HRMS (ESI-TOF): m/z calcd for $\text{C}_{23}\text{H}_{31}\text{N}_5\text{O}$ $[\text{M}+\text{H}]^+$ 394.2601, found 394.2603.

4.1.5.32.3-(3-Chlorobenzyl)-2-(thiophen-2-yl)-7-(piperazin-1-yl)-3H-imidazo[4,5-b]pyridine
acetate (**32**)

Pale yellow solid, overall yield 35%,; UHPLC-UV purity 99.2% (220 nm); $\text{C}_{23}\text{H}_{24}\text{ClN}_5\text{O}_2\text{S}$, MW 469.99. ^1H NMR (500 MHz, DMSO- d_6) δ ppm: 1.80 (s, 3H), 3.04 (br. s., 4H), 3.98 (br. s., 4H), 5.67 (s, 2H), 6.39 (d, $J = 7.5$ Hz, 1H), 6.61 (d, $J = 5.7$ Hz, 1H), 7.07–7.12 (m, 1H), 7.15 (t, $J = 7.7$ Hz, 1H), 7.22 (d, $J = 3.4$ Hz, 1H), 7.28 (t, $J = 7.7$ Hz, 1H), 7.54 (d, $J = 8.0$ Hz, 1H), 7.70 (d, $J = 5.2$ Hz, 1H), 7.94 (d, $J = 5.7$ Hz, 1H). ^{13}C NMR (125 MHz, DMSO- d_6) δ ppm: 21.7, 44.6, 44.7, 47.2, 103.4, 124.2, 127.0, 127.7, 128.3, 128.9, 129.7, 130.0, 130.2, 131.6, 132.3, 134.5, 143.7, 145.9, 147.2, 150.1, 172.6. HRMS (ESI-TOF): m/z calcd for $\text{C}_{21}\text{H}_{20}\text{ClN}_5\text{S}$ $[\text{M}+\text{H}]^+$ 410.1201, found 410.1205.

4.1.5.33. 3-(3-Fluorobenzyl)-2-(4-fluorophenyl)-7-(piperazin-1-yl)-3H-imidazo[4,5-b]pyridine hydrochloride (**33**)

White solid, overall yield 36 %; UHPLC-UV purity 99.0% (220 nm); C₂₃H₂₂ClF₂N₅, MW 441.91. ¹H NMR (500 MHz, DMSO-*d*₆) δ ppm: 3.30 (br. s., 4H), 4.47 (br. s., 4H), 5.82 (s, 2H), 6.75 (d, *J* = 7.8 Hz, 1H), 6.88 (d, *J* = 9.9 Hz, 1H), 7.00 (d, *J* = 6.7 Hz, 1H), 7.08 (dt, *J* = 2.6, 8.6 Hz, 1H), 7.30 (dt, *J* = 6.0, 7.9 Hz, 1H), 7.35–7.42 (m, 2H), 7.72–7.79 (m, 2H), 8.19 (d, *J* = 7.3 Hz, 1H), 9.82 (br. s., 2H). ¹³C NMR (125 MHz, DMSO-*d*₆) δ ppm: 42.3, 44.6, 47.1, 102.8, 113.6 (d, *J* = 23.0 Hz), 114.7 (d, *J* = 21.0 Hz), 116.1 (d, *J* = 22.0 Hz), 122.4 (d, *J* = 2.9 Hz), 123.1, 125.1 (d, *J* = 3.0 Hz), 130.9, 131.0, 131.6 (d, *J* = 8.6 Hz), 138.5, 138.6, 148.6, 148.7, 162.2 (d, *J* = 244.0 Hz), 163.3 (d, *J* = 249.0 Hz). HRMS (ESI-TOF): *m/z* calcd for C₂₃H₂₁F₂N₅ [M+H]⁺ 406.1838, found 406.1840.

4.1.5.34. 3-(3-Fluorophenethyl)-7-(piperazin-1-yl)-3H-imidazo[4,5-b]pyridine hydrochloride (**34**)

White solid, overall yield 31 %, UHPLC-UV purity 98.0% (220 nm); C₁₈H₂₁ClFN₅, MW 361.85. ¹H NMR (500 MHz, DMSO-*d*₆) δ ppm: 3.15 (t, *J* = 7.5 Hz, 2H), 3.25 (br. s., 4H), 4.24–4.63 (m, 4H), 4.65–4.71 (m, 2H), 6.95 (d, *J* = 6.9 Hz, 1H), 7.01 (td, *J* = 8.6, 2.3 Hz, 1H), 7.10 (d, *J* = 7.5 Hz, 1H), 7.21–7.32 (m, 2H), 8.16 (d, *J* = 6.9 Hz, 1H), 8.31 (s, 1H), 9.81 (br. s., 2H). ¹³C NMR (125 MHz, DMSO-*d*₆) δ ppm: 35.4, 42.8, 45.1, 46.3, 102.4, 114.0, 114.2, 116.3, 116.5, 123.8, 125.8, 130.8, 130.8, 136.2, 140.7, 140.7, 141.6, 150.0, 161.7, 163.6. HRMS (ESI-TOF): *m/z* calcd for C₁₈H₂₀FN₅ [M+H]⁺ 326.1776, found 326.1777.

4.1.5.35. 3-(3-Chlorophenethyl)-7-(piperazin-1-yl)-3H-imidazo[4,5-b]pyridine hydrochloride (**35**)

White solid, overall yield 35 %; UHPLC-UV purity 99.0% (220 nm); C₁₈H₂₁Cl₂N₅, MW 378.30. ¹H NMR (500 MHz, DMSO-*d*₆) δ ppm: 3.13 (t, *J* = 7.7 Hz, 2H), 3.25 (br. s., 4H), 4.11–4.59 (m, 4H), 4.65 (t, *J* = 7.5 Hz, 2H), 6.92 (d, *J* = 6.9 Hz, 1H), 7.14–7.34 (m, 3H), 7.42 (s, 1H), 8.15 (d, *J* = 6.9 Hz, 1H), 8.30 (s, 1H), 9.77 (br. s., 2H). ¹³C NMR (125 MHz, DMSO-*d*₆) δ ppm: 35.3, 42.8, 45.1, 45.1, 46.1, 102.5, 123.9, 127.2, 128.3, 129.5, 130.8, 133.5, 140.5, 141.6. HRMS (ESI-TOF): *m/z* calcd for C₁₈H₂₀ClN₅ [M+H]⁺ 342.1480, found 342.1484.

4.1.5.36. 3-(3-Chlorophenethyl)-2-methyl-7-(piperazin-1-yl)-3H-imidazo[4,5-b]pyridine hydrochloride (**36**)

White solid, overall yield 38 %; UHPLC-UV purity 99.2% (220 nm); C₁₉H₂₃Cl₂N₅, MW 392.33. ¹H NMR (500 MHz, DMSO-*d*₆) δ ppm: 2.38 (s, 3H), 3.04 (s, 2H), 3.25 (br. s., 4H), 4.17–4.53 (m, 4H), 4.57 (s, 2H), 6.86–6.94 (m, 1H), 7.17–7.24 (m, 1H), 7.24–7.32 (m, 2H), 7.40 (s, 1H), 8.09 (d,

$J = 6.9$ Hz, 1H). ^{13}C NMR (125 MHz, DMSO- d_6) δ ppm: 13.7, 34.7, 42.8, 45.1, 45.3, 127.3, 128.5, 129.7, 130.8, 133.5, 140.5, 149.8. HRMS (ESI-TOF): m/z calcd for $\text{C}_{19}\text{H}_{22}\text{ClN}_5$ $[\text{M}+\text{H}]^+$ 356.1636, found 356.1633.

4.1.5.37. 3-(3-Fluorophenethyl)-2-ethyl-7-(piperazin-1-yl)-3H-imidazo[4,5-b]pyridine
hydrochloride (**37**)

White solid, overall yield 30 %; UHPLC-UV purity 99.0% (220 nm); $\text{C}_{20}\text{H}_{25}\text{ClFN}_5$, MW 389.90. ^1H NMR (500 MHz, DMSO- d_6) δ ppm: 1.20 (t, $J = 7.5$ Hz, 3H), 2.67 (q, $J = 7.5$ Hz, 2H), 3.05 (t, $J = 7.5$ Hz, 2H), 3.25 (br. s., 4H), 4.41 (br. s., 4H), 4.58 (t, $J = 7.7$ Hz, 2H), 6.92 (d, $J = 7.5$ Hz, 1H), 6.98–7.05 (m, 1H), 7.07 (d, $J = 8.0$ Hz, 1H), 7.22 (d, $J = 9.7$ Hz, 1H), 7.28 (td, $J = 7.7, 6.3$ Hz, 1H), 8.09 (d, $J = 7.5$ Hz, 1H), 9.75 (br. s., 2H). ^{13}C NMR (125 MHz, DMSO- d_6) δ ppm: 11.4, 20.0, 34.9, 41.0, 42.8, 45.1, 102.8, 114.0, 114.2, 116.5, 116.7, 125.9, 130.8, 130.8, 140.7, 140.8, 153.8, 161.7, 163.6. HRMS (ESI-TOF): m/z calcd for $\text{C}_{20}\text{H}_{24}\text{FN}_5$ $[\text{M}+\text{H}]^+$ 354.2089, found 354.2090.

4.1.5.38. 3-(3-Chlorophenethyl)-2-ethyl-7-(piperazin-1-yl)-3H-imidazo[4,5-b]pyridine
hydrochloride (**38**)

White solid, overall yield 32%, UHPLC-UV purity 98.6% (220 nm); $\text{C}_{20}\text{H}_{25}\text{Cl}_2\text{N}_5$, MW 406.36. ^1H NMR (500 MHz, DMSO- d_6) δ ppm: 1.20 (t, $J = 7.5$ Hz, 3H), 2.69 (q, $J = 7.5$ Hz, 2H), 3.03 (t, $J = 7.5$ Hz, 2H), 3.25 (br. s., 4H), 4.16–4.52 (m, 4H), 4.56 (t, $J = 7.5$ Hz, 2H), 6.90 (d, $J = 7.5$ Hz, 1H), 7.19–7.24 (m, 1H), 7.24–7.30 (m, 2H), 7.39 (s, 1H), 8.08 (d, $J = 6.9$ Hz, 1H), 9.74 (br. s., 2H). ^{13}C NMR (125 MHz, DMSO- d_6) δ ppm: 11.4, 20.1, 34.8, 41.0, 42.8, 44.9, 45.1, 102.8, 127.3, 128.5, 129.6, 130.7, 133.5, 140.5, 153.7. HRMS (ESI-TOF): m/z calcd for $\text{C}_{20}\text{H}_{24}\text{ClN}_5$ $[\text{M}+\text{H}]^+$ 370.179, found 370.1794.

4.1.5.39. 3-(3-Chlorophenethyl)-2-isopropyl-7-(piperazin-1-yl)-3H-imidazo[4,5-b]pyridine
hydrochloride (**39**)

Yellow solid, overall yield 34 %; UHPLC-UV purity 98.4% (220 nm); $\text{C}_{21}\text{H}_{27}\text{Cl}_2\text{N}_5$, MW 420.38. ^1H NMR (500 MHz, DMSO- d_6) δ ppm: 1.03–1.22 (m, 6H), 2.97 (dt, $J = 13.8, 6.9$ Hz, 1H), 3.04 (t, $J = 7.5$ Hz, 2H), 3.25 (br. s., 4H), 4.40 (d, $J = 1.7$ Hz, 4H), 4.58 (t, $J = 7.2$ Hz, 2H), 6.91 (d, $J = 6.9$ Hz, 1H), 7.14–7.19 (m, 1H), 7.22–7.28 (m, 2H), 7.32 (s, 1H), 8.10 (d, $J = 6.9$ Hz, 1H), 9.70 (br. s., 2H). ^{13}C NMR (125 MHz, DMSO- d_6) δ ppm: 21.8, 26.1, 35.1, 42.8, 44.8, 45.2, 102.8, 123.1, 127.3, 128.5, 129.6, 130.8, 133.6, 140.4, 157.3. HRMS (ESI-TOF): m/z calcd for $\text{C}_{21}\text{H}_{26}\text{ClN}_5$ $[\text{M}+\text{H}]^+$ 384.1950, found 384.1951.

4.2. *In vitro* pharmacology

4.2.1. Radioligand binding assays

All the experiments were carried out according to the previously published procedures [27–30], using [³H]-8-OH-DPAT (135.2 Ci/mmol), [³H]-Ketanserin (53.4 Ci/mmol), [³H]-LSD (83.6 Ci/mmol), [³H]-5-CT (80.1 Ci/mmol) and [³H]-Raclopride (76.0 Ci/mmol) for 5-HT_{1A}, 5-HT_{2A}, 5-HT₆, 5-HT_{7B} and D₂, respectively. Non-specific binding is defined with 10 μM of 5-HT in 5-HT_{1A}R and 5-HT_{7R} binding experiments, whereas 10 μM of chlorpromazine, 10 μM of methiothepine or 10 μM of haloperidol were used in 5-HT_{2A}R, 5-HT₆R and D_{2L} assays, respectively. Each compound was tested in triplicate at 7–8 concentrations (10⁻¹¹–10⁻⁴ M). The inhibition constants (*K_i*) were calculated from the Cheng-Prusoff equation [31].

HEK293 cells with stable expression of human serotonin 5-HT_{1A}R, 5-HT₆R, 5-HT_{7b}R or dopamine D_{2L}R (all prepared with the use of Lipofectamine 2000) were maintained at 37 °C in a humidified atmosphere with 5% CO₂ and were grown in Dulbecco's Modifier Eagle Medium containing 10% dialysed foetal bovine serum and 500 mg/mL G418 sulphate. For membranes preparations, cells were subcultured in 150 cm² flasks, grown to 90% confluence, washed twice with prewarmed to 37°C phosphate buffered saline (PBS) and were pelleted by centrifugation (200 g) in PBS containing 0.1 mM EDTA and 1 mM dithiothreitol. Prior to membrane preparations pellets were stored at –80°C. CHO-K1 cells with stable expression of human serotonin 5-HT_{2A}R were purchased from PerkinElmer BioSignal Inc and were maintained according to manufacturer's protocol.

Cell pellets were thawed and homogenized in 20 volumes of assay buffer using an Ultra Turrax tissue homogenizer and centrifuged twice at 35 000 g for 20 min at 4°C, with incubation for 15 min at 37°C in between. The composition of the assay buffers was as follows: for 5-HT_{1A}R: 50 mM Tris–HCl, 0.1 mM EDTA, 4 mM MgCl₂, 10 μM pargyline and 0.1% ascorbate; for 5-HT_{2A}R: 50 mM Tris–HCl, 0.1 mM EDTA, 4 mM MgCl₂ and 0.1% ascorbate; for 5-HT₆R: 50 mM Tris–HCl, 0.5 mM EDTA and 4 mM MgCl₂, for 5-HT_{7b}R: 50 mM Tris–HCl, 4 mM MgCl₂, 10 μM pargyline and 0.1% ascorbate; for dopamine D_{2L}R: 50 mM Tris–HCl, 1 mM EDTA, 4 mM MgCl₂, 120 mM NaCl, 5 mM KCl, 1.5 mM CaCl₂ and 0.1% ascorbate.

All assays were incubated in a total volume of 200 μL in 96-well microtitre plates for 1 h at 37°C, except for 5-HT_{1A}R and 5-HT_{2A}R which were incubated at room temperature for 1 h and 1.5 h, respectively. The process of equilibration is terminated by rapid filtration through Unifilter plates with a 96-well cell harvester and radioactivity retained on the filters was quantified on a Microbeta plate reader.

Additionally, the percentage of inhibition for compound **17** for adrenergic α_1R , dopaminergic D_3Rs , histamine H_1 and H_3Rs , muscarinic M_1 , hERG potassium channel as well as for monoamine transporter SERT, were evaluated at Eurofins Cerep according to experimental conditions described online at www.cerep.fr.

4.2.2. Determination of cAMP production as 5-HT₆R constitutive activity

cAMP measurement was performed in NG108-15 cells transiently expressing 5-HT₆R using the bioluminescence resonance energy transfer (BRET) sensor for cAMP, CAMYEL (cAMP sensor using YFP-Epac-RLuc) [31]. NG108-15 cells were co-transfected in suspension with 5-HT₆R and CAMYEL constructs, using Lipofectamine 2000, according to the manufacturer's protocol, and plated in white 96-well plates (Greiner), at a density of 80 000 cells per well. Twenty-four h after transfection, cells were washed with PBS containing calcium and magnesium. Coelenterazine H (Molecular Probes) was added at a final concentration of 5 μ M, and left at room temperature for 5 min. BRET was measured using a Mithras LB 940 plate reader (Berthold Technologies). Expression of 5-HT₆R in NG-108-15 cells induced a strong decrease in CAMYEL BRET signal, compared with cells transfected with an empty vector instead of the plasmid encoding the 5-HT₆R. This decrease in CAMYEL BRET signal was thus used as an index of 5-HT₆R constitutive activity at Gs signaling.

4.3. In vitro evaluation of Cdk5 protein kinase activity

NG108-15 cells were grown in Dulbecco's modified Eagle's medium (DMEM) supplemented with 10% dialyzed foetal calf serum, 2% hypoxanthine/aminopterin/thymidine (Life technologies), and antibiotics. Cells were transfected with plasmids encoding either cytosolic GFP or a GFP-tagged 5-HT₆ receptor in suspension using Lipofectamine 2000 (Life technologies) and plated on glass coverslips. Six hours after transfection, cells were treated with either DMSO (control), or compound **17** or intepirdine (1 μ M) for 24 h. Cells were fixed in 4% paraformaldehyde (PFA) supplemented with 4% sucrose for 10 min. PFA fluorescence was quenched by incubating the cells in PBS containing 0,1M Glycine, prior to mounting in Prolong Gold antifade reagent (Thermo Fisher Scientific). Cells were imaged using an AxioImagerZ1 microscope equipped with epifluorescence (Zeiss), using a 20 X objective for cultured cells and neurite length was assessed using the Neuron J plugin of the ImageJ software (NIH).

4.4. In vitro evaluation of interaction with cytochrome P450

The evaluation of the influence of tested compound **17** on cytochrome P-450 isoforms activity was performed using luminescence assay basing on the conversion of luciferin derivatives into D-luciferin by recombinant CYPs. The luminescent CYP3A4 P450-Glo™ and CYP2D6 P450-Glo™ assays and protocols were provided by Promega (Madison, WI, USA) (Cali JJ, Ma D, Sobol M, et al. Luminogenic cytochrome P450 assays. *Expert Opin Drug Metab Toxicol.* 2006;2:629–645). The reference drugs ketoconazole and quinidine were obtained from Sigma-Aldrich (St. Louis, USA). The enzymatic reactions were performed in white polystyrene, flat-bottom Nunc™ MicroWell™ 96-Well Microplates (Thermo Scientific, Waltham, MA USA). The luminescence signal was measured with a microplate reader in luminescence mode (EnSpire, PerkinElmer, Waltham, MA USA). The cytochrome P-450 isoform 3A4 or 2D6 were incubated for two hour in the presence of examined compounds and luciferin derivative, specific for particular CYP isoform. After addition of the firefly luciferase, the amount of light produced in bioluminescent reaction will be proportional to the amount of D-luciferin obtained in CYP-catalyzed reaction allowing to assess the effect of examined compound on CYPs activity. The IC₅₀ value of the reference drug ketoconazole was determinate and calculated as reported previously [32]. The IC₅₀ value of the reference drug quinidine was determined according to the manufacturer's recommendations at the final concentrations of quinidine 0.1–100 nM. The final concentrations of tested compound were similar for both CYP3A4 and 2D6 assays and were from 0.025 μM to 25 μM. The IC₅₀ values were calculated as the measurement of inhibition potency of tested compounds and then compared with reference inhibitors of each CYP's isoform.

4.5. *In vitro* metabolic stability studies

Test compound incubation (10 μM) with RLM (0.2 mg/mL) was performed in 100 mM potassium phosphate buffer (PB), pH 7.4, at 37°C for 15 min in a final reaction mixture volume of 150 μl. The reaction was initiated by the addition of an NADPH-regenerating system (NADP, glucose-6-phosphate, glucose-6-phosphate dehydrogenase in 100 mM PB, pH 7.4) to the incubation mixture. The blank probe without the NADPH – regenerating system was performed in parallel [33,34]. Subsequently, the samples were incubated at 37°C for 5, 15, 30 min with gentle shaking. Next, an internal standard (pentoxiphylline, 5 μM) was added. The reaction was terminated at different time points with perchloric acid (69-72%, by volume). Thereafter, all samples were centrifuged and the supernatant was analyzed using UPLC/MS in order to determine the quantity of starting material left in solution. All samples were prepared in duplicate.

The *in vitro* half-time ($t_{1/2}$) for test compounds was determined from the slope of the linear regression of \ln % parent compound remaining versus incubation time. The calculated $t_{1/2}$ was incorporated into the following equation to obtain intrinsic clearance (Cl_{int}) = (volume of incubation [ml]/ protein in the incubation [kg]) \times 0.693/ $t_{1/2}$.

4.6. Preliminary *in vivo* pharmacokinetic experiments

The care, use of the animals and the experimental protocols was approved by the Local Bioethical Committee in Białystok. Pharmacokinetic experiment was carried out on male Wistar rats, 229 – 272 g (Center for Experimental Medicine, University of Białystok, Białystok, Poland). Before the experiment, rats were deprived of food for 16 hours (water *ad libitum*) before and 4 h after administration. The compound formulated in water was administered orally in a dose of 10 mg/kg b.w. Total of 24 animals (4 per timepoint) were used for each sampling timepoint at 15 min, 30 min, 1h, 2h, 4h and 8h after administration. Blood was collected by cardiac puncture and subsequently brains were removed. Blood samples were collected with K3EDTA as anticoagulant and centrifuged (3000g, 15 min, 4°C). The obtained blood plasma was separated and stored at -20°C until used for analysis. Subsequently, brains were removed, washed with cold saline, homogenized in water (3ml/1 mg of brain tissue) and stored at -80°C until used for analysis. Blood and brain samples were analysed by liquid chromatography–tandem mass spectrometry systems: Agilent Technologies 6460 Triple Quad and LC/MS Sciex QTrap 4500, respectively.

4.7. *In vitro* anti-mutagenicity assay (Ames test)

Ames microplate fluctuation protocol (MPF) assay was performed with *Salmonella typhimurium* strains TA98 and TA100, enabling the detection of both: frame shift and base substitution mutations, respectively. Bacterial strains as well as exposure and indicator medium were purchased from Xenometrix AG (Allschwil, Switzerland). The mutagenic potential of tested compound was evaluated by incubation of bacteria, incapable of producing histidine, with particular concentration of test compounds for 90 min in exposure medium, containing limited amount of histidine. The occurrence of reversion events to histidine prototrophy was observed as a growth of bacteria in the indicator medium without histidine after 48 h of incubation in room temperature. Bacterial growth in 384-well plates was visualized by color change of medium from violet to yellow due to addition of pH indicator dye. Compound was classified as mutagenic, if the fold increase in number of positive wells over the solvent control baseline (FIB) was greater than 2.0. The FIB was determined

by dividing the mean number of revertants for tested compound by the solvent control baseline. The solvent control baseline was defined as the mean number of positive wells in the negative control sample, increased by one standard deviation (SD). DMSO was used as a negative and 4-nitroquinoline N-oxide (NQNO) as positive control in performed experiments.

4.8. *In vivo behavioral evaluation*

The experiments were performed according to the previously reported procedures [35], and were conducted in accordance with the NIH Guide for the Care and Use of Laboratory Animals and were approved by the Ethics Committee for Animal Experiments, Institute of Pharmacology. Male Sprague–Dawley rats (Charles River, Germany) weighing ~150 g at the arrival were housed in the standard laboratory cages, under standard colony A/C controlled conditions: room temperature $21 \pm 2^\circ\text{C}$, humidity (40–50 %), 12-hr light/dark cycle (lights on: 06:00) with ad libitum access to food and water. Rats were allowed to acclimatize for at least 7 days before the start of the experimental procedure. During this week animals were handled for at least 3 times. Behavioral testing was carried out during the light phase of the light/dark cycle. At least 1 h before the start of the experiment, rats were transferred to the experimental room for acclimation. Rats were tested in a dimly lit (25 lx) “open field” apparatus made of a dull gray plastic ($66 \times 56 \times 30$ cm). After each measurement, the floor was cleaned and dried.

4.8.1. *Drug treatment*

Phencyclidine, scopolamine and intepirdine (SB-742457) were obtained from Sigma–Aldrich (Poznan, Poland) while donepezil from Abcam, (UK). Phencyclidine and scopolamine, used to attenuate learning, were solubilized in distilled water and were administered at the dose of 5 mg/kg (*i.p.*) and 1.25 mg/kg (*i.p.*) 45 and 30 min before familiarization phase (T1), respectively. Tested compound **17** and donepezil was administrated *p.o.* 120 min before familiarization phase (T1). In contrast to compound **17**, donepezil was studied only in scopolamine-induced memory impairment paradigm in order to study the interaction combined treatment of compound **17** with donepezil, both administered in inactive doses.

4.8.2. *Experimental procedure*

Procedure consisted of habituation to the arena (without any objects) for 5 min, 24 hours before the test and test session comprised of two trials separated by an inter trial interval (ITI). For

phencyclidine (PCP) or scopolamine (SCOP)-induced memory impairment paradigm, 1 hour ITI was chosen. During the first trial (familiarization, T1) two identical objects (A1 and A2) were presented in opposite corners, approximately 10 cm from the walls of the open field. In the second trial (recognition, T2) one of the objects was replaced by a novel one (A = familiar and B = novel). Both trials lasted 3 min and animals were returned to their home cage after T1. The objects used were the glass beakers filled with the gravel and the plastic bottles filled with the sand. The heights of the objects were comparable (~12 cm) and the objects were heavy enough not to be displaced by the animals. The sequence of presentations and the location of the objects was randomly assigned to each rat. The animals explored the objects by looking, licking, sniffing or touching the object while sniffing, but not when leaning against, standing or sitting on the object. Any rat spending less than 5 s exploring the two objects within 3 min of T1 or T2 was eliminated from the study. Exploration time of the objects and the distance traveled were measured using the Any-maze® video tracking system. Based on exploration time (E) of two objects during T2, discrimination index (DI) was calculated according to the formula: $DI = (EB - EA) / (EA + AB)$. Because the analyses of exploration time during recognition trial and DI yielded the same results, only DI data were presented.

4.8.3. Statistics

Data on exploratory preference and distance travelled were analyzed using two-way repeated measures ANOVAs with trial as repeated factor; DI data were analyzed by one-way ANOVA followed by Newman-Keuls post hoc test.

Acknowledgements

This project was supported from the statutory activity of Jagiellonian University Medical College, by the grants PBS3/B7/20/2015 from the Polish National Centre for Research and Development, 17-31834A (Ministry of Health of the Czech Republic) and LO1304 (Czech National Sustainability Program). PM and SCD were supported by grants from CNRS, INSERM, University of Montpellier, Pôle Biosanté Rabelais, Fondation pour la Recherche Médicale and ANR (contracts n°ANR-17-CE16-0013-01 to PM and n°ANR-17-CE16-0010 to SCD). We thank Mr Mikołaj Matłoka and dr Jerzy Pieczykolan from Celon Pharma Ltd for providing us with pharmacokinetic experiments.

References:

- [1] H.M. Yun, S. Kim, H.J. Kim, E. Kostenis, J. Il Kim, J.Y. Seong, J.H. Baik, H. Rhim, The novel cellular mechanism of human 5-HT₆ receptor through an interaction with Fyn., *J. Biol. Chem.* 282 (2007) 5496–5505.
- [2] J. Meffre, S. Chaumont-Dubel, C. Mannoury la Cour, F. Loiseau, D.J.G. Watson, A. Dekeyne, M. Seveno, J.M. Rivet, F. Gaven, P. Deleris, D. Herve, K.C.F. Fone, J. Bockaert, M.J. Millan, P. Marin, 5-HT(6) receptor recruitment of mTOR as a mechanism for perturbed cognition in schizophrenia., *EMBO Mol. Med.* 4 (2012) 1043–1056.
- [3] M. Jacobshagen, M. Niquille, S. Chaumont-Dubel, P. Marin, A. Dayer, The serotonin 6 receptor controls neuronal migration during corticogenesis via a ligand-independent Cdk5-dependent mechanism., *Development.* 141 (2014) 3370–3377.
- [4] N. Upton, T.T. Chuang, A.J. Hunter, D.J. Virley, 5-HT₆ receptor antagonists as novel cognitive enhancing agents for Alzheimer's disease., *Neurotherapeutics.* 5 (2008) 458–469.
- [5] K. Wicke, A. Haupt, A. Bernalov, Investigational drugs targeting 5-HT₆ receptors for the treatment of Alzheimer's disease., *Expert Opin. Investig. Drugs.* 24 (2015) 1515–1528.
- [6] L.P. Lacroix, L.A. Dawson, J.J. Hagan, C.A. Heidbreder, 5-HT₆ receptor antagonist SB-271046 enhances extracellular levels of monoamines in the rat medial prefrontal cortex., *Synapse.* 51 (2004) 158–164.
- [7] A. Tassone, G. Madeo, T. Schirinzi, D. Vita, F. Puglisi, G. Ponterio, F. Borsini, A. Pisani, P. Bonsi, Activation of 5-HT₆ receptors inhibits corticostriatal glutamatergic transmission., *Neuropharmacology.* 61 (2011) 632–637.
- [8] G. Maher-Edwards, M. Zvartau-Hind, A.J. Hunter, M. Gold, G. Hopton, G. Jacobs, M. Davy, P. Williams, Double-blind, controlled phase II study of a 5-HT₆ receptor antagonist, SB-742457, in Alzheimer's disease., *Curr. Alzheimer Res.* 7 (2010) 374–385.
- [9] D. Wilkinson, K. Windfeld, E. Colding-Jorgensen, Safety and efficacy of idalopirdine, a 5-HT₆ receptor antagonist, in patients with moderate Alzheimer's disease (LADDER): a randomised, double-blind, placebo-controlled phase 2 trial., *Lancet. Neurol.* 13 (2014) 1092–1099.
- [10] I.E.M. de Jong, A. Mørk, Antagonism of the 5-HT₆ receptor – Preclinical rationale for the treatment of Alzheimer's disease., *Neuropharmacology.* 125 (2017) 50–63.

- [11] Available online: <https://clinicaltrials.gov/show/NCT02669433>, accessed on September 2017.
- [12] Available online: <https://clinicaltrials.gov/show/NCT02258152>, accessed on August 2017.
- [13] F. Duhr, P. Déléris, F. Raynaud, M. Séveno, S. Morisset-Lopez, C. Mannoury la Cour, M.J. Millan, J. Bockaert, P. Marin, S. Chaumont-Dubel, Cdk5 induces constitutive activation of 5-HT₆ receptors to promote neurite growth., *Nat. Chem. Biol.* 10 (2014) 590–597.
- [14] W.D. Nadim, S. Chaumont-Dubel, F. Madouri, L. Cobret, M.L. De Tauzia, P. Zajdel, H. Bénédicti, P. Marin, S. Morisset-Lopez, Physical interaction between neurofibromin and serotonin 5-HT₆ receptor promotes receptor constitutive activity., *Proc. Natl. Acad. Sci. U.S.A.* 43 (2016) 12310–12315.
- [15] B. Benhamú, M. Martin-Fontecha, H. Vazquez-Villa, L. Pardo, M.L. Lopez-Rodriguez, Serotonin 5-HT₆ receptor antagonists for the treatment of cognitive deficiency in Alzheimer's disease., *J. Med. Chem.* 57 (2014) 7160–7181.
- [16] R.A. Glennon, U. Siripurapu, B.L. Roth, R. Kolanos, M.L. Bondarev, D. Sikazwe, M. Lee, M. Dukat, The medicinal chemistry of 5-HT₆ receptor ligands with a focus on arylsulfonyltryptamine analogs., *Curr. Top. Med. Chem.* 10 (2010) 579–595.
- [17] J. Holenz, P.J. Pauwels, J.L. Diaz, R. Merce, X. Codony, H. Buschmann, Medicinal chemistry strategies to 5-HT(6) receptor ligands as potential cognitive enhancers and antiobesity agents., *Drug Discov. Today.* 11 (2006) 283–299.
- [18] P. Zajdel, K. Marciniak, G. Satała, V. Canale, T. Kos, A. Partyka, M. Jastrzębska-Więsek, A. Wesołowska, A. Basińska-Ziobron, J. Wojcikowski, W.A. Daniel, A.J. Bojarski, P. Popik, N₁-Azinylsulfonyl-1*H*-indoles: 5-HT₆ Receptor antagonists with procognitive and antidepressant-like properties., *ACS Med. Chem. Lett.* 7 (2016) 618–622.
- [19] D.C. Kelly, M.G. Cole, 1-Aryl or 1-alkylsulfonyl-heterocyclyl-benzazoles as 5-hydroxytryptamine-6-ligands, WO Patent 2002036562, 2006.
- [20] A.J. Haydar, S.M. Andrae, P.M. Yun, H. Robichaud, 1-(Arylsulfonyl)-4-(piperazin-1-yl)-1*H*-benzimidazoles as 5-hydroxytryptamine-6-ligands, US Patent 2010120779, 2010.
- [21] D.C. Cole, W.J. Lennox, J.R. Stock, J.W. Ellingboe, H. Mazandarani, D.L. Smith, G. Zhang, G.J. Tawa, L.E. Schechter, Conformationally constrained N₁-arylsulfonyltryptamine

- derivatives as 5-HT₆ receptor antagonists., *Bioorg. Med. Chem. Lett.* 15 (2005) 4780–4785.
- [22] R. Nirogi, A. Shinde, R.S. Kambhampati, A.R. Mohammed, S.K. Saraf, R.K. Badange, T.R. Bandyala, V. Bhatta, K. Bojja, V. Reballi, R. Subramanian, V. Benade, R.C. Palacharla, G. Bhyrapuneni, P. Jayarajan, V. Goyal, V. Jasti, Discovery and development of 1-[(2-Bromophenyl)sulfonyl]-5-methoxy-3-[(4-methyl-1-piperazinyl)methyl]-1H-indole dimesylate monohydrate (SUVN-502): a novel, potent, selective and orally active serotonin 6 (5-HT₆) receptor antagonist for potential treatment, *J. Med. Chem.* 60 (2017) 1843–1859.
- [23] B. Lemrova, P. Smyslova, I. Popa, T. Ozdian, P. Zajdel, M. Soural, Directed solid-phase synthesis of trisubstituted imidazo[4,5-*c*]pyridines and imidazo[4,5-*b*]pyridines., *ACS Comb. Sci.* 16 (2014) 558–565.
- [24] A. Ennaceur, J. Delacour, A new one-trial test for neurobiological studies of memory in rats. 1: Behavioral data., *Behav. Brain Res.* 31 (1988) 47–59.
- [25] K. Grychowska, G. Satała, T. Kos, A. Partyka, E. Colacino, S. Chaumont-Dubel, X. Bantreil, A. Wesołowska, M. Pawłowski, J. Martinez, P. Marin, G. Subra, A.J. Bojarski, F. Lamaty, P. Popik, P. Zajdel, Novel 1*H*-pyrrolo[3,2-*c*]quinoline based 5-HT₆ receptor antagonists with potential application for the treatment of cognitive disorders associated with Alzheimer's disease., *ACS Chem. Neurosci.* 7 (2016) 972–983.
- [26] A. Atri, G. Tong, J. Isojarvi, T. Odergren, A 5-HT₆ Antagonist as adjunctive therapy to cholinesterase inhibitors in patients with mild-to-moderate Alzheimer's disease: Idalopirdine in Phase III (PL02.006), *Neurol.* 86 (2016).
- [27] A.J. Bojarski, M.T. Cegla, S. Charakchieva-Minol, M.J. Mokrosz, M. Maćkowiak, S. Misztal, J.L. Mokrosz, Structure-activity relationship studies of CNS agents. Part 9: 5-HT_{1A} and 5-HT₂ receptor affinity of some 2- and 3-substituted 1,2,3,4-tetrahydro-beta-carbolines., *Pharmazie.* 48 (1993) 289–294.
- [28] M.H. Paluchowska, R. Bugno, B. Duszyńska, E. Tatarczyńska, A. Nikiforuk, T. Lenda, E. Chojnacka-Wójcik, The influence of modifications in imide fragment structure on 5-HT(1A) and 5-HT(7) receptor affinity and *in vivo* pharmacological properties of some new 1-(*m*-trifluoromethylphenyl)piperazines., *Bioorg. Med. Chem.* 15 (2007) 7116–7125.
- [29] P. Zajdel, K. Marciniak, A. Maslankiewicz, G. Satała, B. Duszyńska, A.J. Bojarski, A. Partyka, M. Jastrzębska-Więsek, D. Wróbel, A. Wesołowska, M. Pawłowski, Quinoline-

and isoquinoline-sulfonamide derivatives of LCAP as potent CNS multi-receptor-5-HT_{1A}/5-HT_{2A}/5-HT₇ and D₂/D₃/D₄-agents: the synthesis and pharmacological evaluation., *Bioorg. Med. Chem.* 20 (2012) 1545–1556.

- [30] P. Zajdel, R. Kurczab, K. Grychowska, G. Satała, M. Pawłowski, A.J. Bojarski, The multiobjective based design, synthesis and evaluation of the arylsulfonamide/amide derivatives of aryloxyethyl- and arylthioethyl- piperidines and pyrrolidines as a novel class of potent 5-HT(7) receptor antagonists., *Eur. J. Med. Chem.* 56 (2012) 348–360.
- [31] Y. Cheng, W.H. Prusoff, Relationship between the inhibition constant (K₁) and the concentration of inhibitor which causes 50 per cent inhibition (I₅₀) of an enzymatic reaction., *Biochem. Pharmacol.* 22 (1973) 3099–3108.
- [32] D. Łazewska, M. Wiecek, J. Ner, K. Kamińska, T. Kottke, J.S. Schwed, M. Zygmunt, T. Karcz, A. Olejarz, K. Kuder, G. Łatacz, M. Grosicki, J. Sapa, J. Karolak-Wojciechowska, H. Stark, K. Kiec-Kononowicz, Aryl-1,3,5-triazine derivatives as histamine H₄ receptor ligands., *Eur. J. Med. Chem.* 83 (2014) 534–546.
- [33] J. Huang, L. Si, Z. Fan, L. Hu, J. Qiu, G. Li, *In vitro* metabolic stability and metabolite profiling of TJ0711 hydrochloride, a newly developed vasodilatory β-blocker, using a liquid chromatography-tandem mass spectrometry method, *J. Chromatogr. B. Analyt. Technol. Biomed. Life Sci.* 879 (2011) 3386–3392.
- [34] L. Di, E.H. Kerns, Y. Hong, T.A. Kleintop, O.J. McConnell, D.M. Huryn, Optimization of a higher throughput microsomal stability screening assay for profiling drug discovery candidates., *J. Biomol. Screen.* 8 (2003) 453–462.
- [35] P. Popik, M. Hołuj, A. Nikiforuk, T. Kos, R. Trullas, P. Skolnick, 1-aminocyclopropanecarboxylic acid (ACPC) produces procognitive but not antipsychotic-like effects in rats., *Psychopharmacology (Berl)*. 232 (2015) 1025–1038.

Highlights

- Novel ligands affecting constitutive activity of 5-HT₆ receptor
- Solid-phase synthesis of new 3*H*-imidazo[4,5-*c*]pyridines and imidazo[4,5-*c*]pyridines
- Intepirdine (SB-742457) prevents 5-HT₆R-elicited neurite growth and behaves as inverse agonist of cyclin-dependent kinase 5 (Cdk5)
- Compound **17** is partial inverse agonist of 5-HT₆R in G_s signaling with no influence on cyclin-dependent kinase 5 (Cdk5)
- Pro-cognitive properties of **17** in scopolamine- and phencyclidine-induced memory deficits in NOT test
- Combination of **17** and donepezil produced synergistic effect in NOR test